Boron isotopic signatures of melt inclusions from North Iceland reveal recycled material in the Icelandic mantle source

Available online at www.sciencedirect.com

ScienceDirect

Geochimica et Cosmochimica Acta 294 (2021) 273–294

Geochimica et Cosmochimica Acta

www.elsevier.com/locate/gca

Boron isotopic signatures of melt inclusions from North Iceland reveal recycled material in the Icelandic mantle source

Margaret E. Hartley [a,*], Jan C.M. de Hoog [b], Oliver Shorttle [c,d]

[a] Department of Earth and Environmental Sciences, University of Manchester, Oxford Road, Manchester M13 9PL, UK
[b] School of Geosciences, University of Edinburgh, James Hutton Road, Edinburgh EH9 3FE, UK
[c] Department of Earth Sciences, University of Cambridge, Downing Street, Cambridge CB2 3EQ, UK
[d] Institute of Astronomy, University of Cambridge, Madingley Road, Cambridge CB0 3HA, UK

Received 30 January 2020; accepted in revised form 12 November 2020; Available online 21 November 2020

Abstract

Trace element and volatile heterogeneity in the Earth's mantle is influenced by the recycling of oceanic lithosphere through subduction. Oceanic island basalts commonly have high concentrations of volatiles compared to mid-ocean ridge basalts, but the extent to which this enrichment is linked to recycled mantle domains remains unclear. Boron is an ideal tracer of recycled subducted material, since only a small percentage of a recycled component is required to modify the bulk δ^{11}B of the source mantle. Boron isotopic compositions of primary melts thus have potential to trace the fate of recycled subducted material in the deep mantle, and to constrain the lengthscales of lithologic and compositional heterogeneities in diverse tectonic settings.

We present new measurements of volatiles, light elements and boron isotopic ratios in basaltic glasses and melt inclusions that sample the mantle at two endmember spatial scales. Submarine glasses from the Reykjanes Ridge sample long-wavelength mantle heterogeneity on the broad scale of the Iceland plume. Crystal-hosted melt inclusions from the Askja and Bárðarbunga volcanic systems in North Iceland sample short-wavelength mantle heterogeneity close to the plume centre. The Reykjanes Ridge glasses record only very weak along-ridge enrichment in B content approaching Iceland, and there is no systematic variability in δ^{11}B along the entire ridge segment. These observations constrain ambient Reykjanes Ridge mantle to have a δ^{11}B of −6.1‰ (2SD = 1.5‰, 2SE = 0.3‰). The North Iceland melt inclusions have widely variable δ^{11}B between −20.7 and +0.6‰. We screen melt inclusions against influence from crustal contamination, identifying high [B] and low δ^{18}O as fingerprints of assimilation processes. Only the most primitive melt inclusions with MgO ⩾ 8 wt.% reliably record mantle-derived δ^{11}B. In North Iceland, incompatible trace element (ITE)-depleted primitive melt inclusions from Holuhraun record a δ^{11}B of −10.6‰, a signal that has also been seen in melt inclusions from southwest Iceland (Gurenko and Chaussidon, 1997). In contrast, primitive ITE-enriched melt inclusions from nearby Askja volcano record a δ^{11}B of −5.7‰, overlapping with our new constraint on the δ^{11}B of Reykjanes Ridge mantle. Coupled [B], δ^{11}B and δ^{18}O signatures of more evolved melt inclusions from North Iceland are consistent with primary melts assimilating <5–20% of hydrothermally altered basaltic hyaloclastite as they ascend through the upper crust.

Our data reveal the presence of a depleted, low-δ^{11}B and an enriched, higher-δ^{11}B mantle component, both intrinsic to the Icelandic mantle source and distinct from Reykjanes Ridge mantle. Non-modal melting calculations suggest that the enriched and depleted mantle components both contain ~0.085 μg/g B, slightly lower than the 0.10–0.11 μg/g calculated for Reykjanes Ridge mantle. These data are consistent with the Icelandic mantle containing B-depleted dehydrated recycled oceanic lithosphere, in keeping with the low B/Pr of Icelandic melt inclusions in comparison to Reykjanes Ridge glasses or MORB. Our new data provide strong support for the role of recycled subducted lithosphere in melt generation at ocean islands, and high-

* Corresponding author.
E-mail address: margaret.hartley@manchester.ac.uk (M.E. Hartley).

https://doi.org/10.1016/j.gca.2020.11.013

light the need for careful screening of melt inclusion compositions in order to study global volatile recycling in ocean island basalts.

Keywords: Boron isotopes; Volatiles; Basalt; Melt inclusion; Mantle; Crustal assimilation; Iceland

1. INTRODUCTION

The chemical flux of volatile elements from the Earth's interior to its surface environments is governed by partial melting of the mantle followed by magma ascent and eruption. Volatiles are returned to the deep mantle through the tectonic recycling of oceanic lithosphere at subduction zones. Over billion-year residence times in the mantle, this subducted material is stretched and thinned so that its geochemical signature is attenuated, creating lithologic, isotopic and volatile element heterogeneities on a range of lengthscales (Allègre and Turcotte, 1986; Kellogg and Turcotte, 1987). Melting of recycled oceanic lithosphere has long been recognised as generating the compositional variability observed in ocean island and mid-ocean ridge basalts (OIB and MORB), through the lithophile radiogenic isotopic compositions (Sr, Nd, Pb, e.g. White and Hofmann, 1982; White, 1985; Zindler and Hart, 1986; Jackson et al., 2012; Stracke, 2012; White, 2010, 2015) and major and trace element systematics (e.g. Langmuir and Hanson, 1980; Weaver, 1991; Hirschmann and Stolper, 1996; Prytulak and Elliott, 2007; Sobolev et al., 2007; Shorttle and Maclennan, 2011) of erupted basalts. Ocean island basalts commonly have high concentrations of volatiles in comparison to MORB (e.g. Schilling et al., 1980); however, the extent to which this volatile enrichment is linked to recycled mantle domains remains unclear (e.g. Kendrick et al., 2015, and references therein).

Boron is incompatible in silicate minerals (Brenan et al., 1998), and its bulk partitioning behaviour between peridotite minerals and basaltic melt is comparable to that of Pr (Marschall et al., 2017). The depleted mantle has a very low B concentration, and its near-uniform boron isotopic signature of $\delta^{11}B = -7.1 \pm 0.9‰$ (Marschall et al., 2017) is not significantly fractionated during melting or crystallization. In contrast, boron is concentrated in surface reservoirs such as seawater, and is both enriched and isotopically fractionated in sediments and hydrothermally altered oceanic crust and lithospheric mantle (Marschall, 2018, and references therein). Enriched and fractionated lithologies returned to the mantle in subducting slabs include: marine sediments ([B] = 1 to >100 μg/g, $\delta^{11}B$ +2 to +26‰); continental sediments ([B]=50–150 μg/g, $\delta^{11}B$ −13 to −8‰); altered oceanic crust ([B]=10–90 μg/g, $\delta^{11}B$ 0 to +18‰); and oceanic serpentinites ([B] 10–90 μg/g, $\delta^{11}B$ +7 to +40‰) (Vils et al., 2009; De Hoog and Savov, 2018). Boron concentrations and boron isotopic compositions are gradually lowered during progressive dehydration of the subducting slab (e.g. Konrad-Schmolke and Halama, 2014). Nevertheless, the isotopic contrast between potential recycled lithologies and depleted mantle means that only a small percentage of a recycled crustal component may be required to modify significantly the boron isotopic signature of the mantle, making boron isotopes potentially a sensitive tracer of recycled subducted material (De Hoog and Savov, 2018). Boron isotopic compositions of primary melts thus have potential both to trace the fate of recycled subducted material in the deep mantle, and to constrain the lengthscales of lithologic and compositional heterogeneities in diverse tectonic settings.

A number of studies have used B contents and $\delta^{11}B$ ratios of primitive basalt whole-rocks and glasses to characterize recycled components in OIB mantle sources (Ryan et al., 1996; Chaussidon and Jambon, 1994; Chaussidon and Marty, 1995; Tanaka and Nakamura, 2005). However, a major challenge in determining the B isotopic compositions of diverse mantle reservoirs is the propensity of ascending melts to assimilate altered crustal material *en route* to the surface. The isotopic contrast between primary mantle melts, geothermal fluids and hydrothermally altered crustal rocks means that bulk $\delta^{11}B$ in basalts is highly sensitive to even small degrees (<3%) of crustal assimilation.

Crystal-hosted melt inclusions offer the possibility of accessing unmodified melt compositions. Primitive inclusions trapped during the earliest stages of fractional crystallization have the highest likelihood of preserving primary mantle-derived elemental concentrations and isotopic signatures (Gurenko and Chaussidon, 1997; Kobayashi et al., 2004; Maclennan, 2008; Walowski et al., 2019). Furthermore, the host mineral shields the melt inclusion from any further effects of crustal processing, such that the inclusion records the B abundance and $\delta^{11}B$ of the surrounding melt at the time of trapping. Melt inclusion suites trapped over a long crystallization interval therefore offer the potential to track chemical signatures of crustal contamination as crystallization proceeds.

Iceland is an ideal natural laboratory for investigating mantle heterogeneity. Previous workers have inferred the presence of recycled oceanic crust in the Icelandic mantle on the basis of major element, incompatible trace element and radiogenic and stable isotope compositions of erupted basalts (e.g. Fitton et al., 1997; Chauvel and Hémond, 2000; Skovgaard et al., 2001; Kokfelt et al., 2006; Shorttle and Maclennan, 2011; Koornneef et al., 2012). Furthermore, mantle heterogeneity is present both on the 100 km lengthscale of Iceland's active neovolcanic zones (e.g. Wood et al., 1979; Zindler et al., 1979; Hanan and Schilling, 1997; Stracke et al., 2003; Thirlwall et al., 2004; Koornneef et al., 2012; Shorttle et al., 2013) and on the lengthscale of melt supply to a single eruption (e.g. Gurenko and Chaussidon, 1995; Maclennan et al., 2007; Maclennan, 2008; Halldorsson et al., 2008; Winpenny and Maclennan,

2011; Neave et al., 2013). The boron isotopic signature of the Icelandic mantle has previously been estimated at $-11.3 \pm 3.8‰$ (2SD; Gurenko and Chaussidon, 1997), based on measurements of primitive olivine-hosted melt inclusions from Miðfell and Mælifell in the Western Volcanic Zone (WVZ), and from the Reykjanes Peninsula. The WVZ inclusions are typified by low ratios of incompatible trace elements such as La/Yb, which could suggest an association between isotopically light boron and a relatively depleted mantle source. However, it is not known whether low $\delta^{11}B$ signatures are typical of Icelandic basalts, nor whether low $\delta^{11}B$ represents a recycled lithology that is heterogeneously distributed in the Icelandic mantle. Brounce et al. (2012) assumed a $\delta^{11}B$ of $-7.8‰$ for the Icelandic mantle, i.e. within the $-7.1 \pm 0.9‰$ proposed for depleted MORB mantle (DMM; Marschall et al., 2017), based on the least negative $\delta^{11}B$ obtained in their study of plagioclase-hosted melt inclusions from the AD 1783 Laki fissure eruption. However, this value was obtained from a melt inclusion containing just 6.09 wt.% MgO, sufficiently evolved that the melt $\delta^{11}B$ may already have been modified through crustal assimilation. The nature and lengthscale of boron isotopic heterogeneity in the Icelandic mantle therefore remains poorly characterized.

A further consideration is that comparisons of $\delta^{11}B$ values obtained at different laboratories and using various analytical techniques must take into account analytical limitations. The past decade has seen significant developments in the characterization of silicate reference materials for boron isotope analysis, as well as improvements to analytical protocols (Marschall, 2018, and references therein). It has been suggested that measured differences in $\delta^{11}B$ from the 1980s and 1990s are not likely to be significant below the 5‰ level (Marschall, 2018), particularly when compared with more recently acquired data. Therefore, a fundamental outstanding question is whether the existence of an isotopically light component in the Icelandic mantle with $\delta^{11}B$ around $-11‰$ (Gurenko and Chaussidon, 1997) can be verified with new high-precision analyses.

In this work we present new measurements of volatiles (H_2O, CO_2, S, F, Cl), light elements (B, Li), and boron isotopic ratios in two sample suites that sample the mantle at two endmember spatial scales. First, we have studied a suite of olivine- and plagioclase-hosted melt inclusions and glasses from North Iceland. These samples have previously been analysed for their major, trace element and oxygen isotopic compositions (Hartley et al., 2012; Hartley and Thordarson, 2013; Hartley et al., 2013). Importantly, the oxygen isotopic signatures of the most primitive melt inclusions reflect a primitive mantle-like component with $\delta^{18}O$ of $+5.2 \pm 0.2‰$, whereas more evolved melt inclusions and matrix glasses have lower $\delta^{18}O$ values that reflect progressive assimilation of low-$\delta^{18}O$ altered basaltic crust. This sample suite is therefore ideal for identifying and characterizing both mantle-derived and assimilation-modified $\delta^{11}B$ signatures on a single-eruption and rift zone scale. We also present new B, Li and boron isotope data for a suite of basalt glasses from the Reykjanes Ridge south of Iceland (Murton, 1995). Previous studies of elemental, isotopic and redox geochemistry in these samples (Murton et al., 2002; Nichols et al., 2002; Shorttle et al., 2015) reveal systematic long-wavelength mantle heterogeneity on the broad scale of the Iceland plume (Schilling, 1973): glasses recovered north of 61°N at radial distances <600 km from the putative plume centre record increasingly enriched and oxidised geochemical signatures, whereas samples collected ~1200–600 km from the plume provide a reference point for the boron isotopic composition of ambient Reykjanes Ridge mantle. With these datasets we examine the volatile, Li, B and boron isotopic heterogeneity in Icelandic primary melts, and determine the extent to which boron isotopic compositions in Icelandic basalts are controlled by crustal contamination. Our results offer insights into the contribution of deep recycled mantle material to melt production, and hence the lengthscales of volatile element heterogeneity across an ocean island.

2. SAMPLES AND ANALYTICAL METHODS

The samples from North Iceland selected for this study comprise basaltic tephra collected from a suite of eruptions located between the northern edge of Vatnajökull glacier and the central part of the Askja volcanic system (Fig. 1). Sample locations and eruption ages are summarized in Table S2.1. The Holuhraun samples discussed in this study were probably erupted between the 1860s and 1890s, and are geochemically similar to melts from the Bárðarbunga volcanic system (Hartley and Thordarson, 2013). These older lavas are now partly covered by the 2014–2015 Holuhraun lava flow field (Pedersen et al., 2017). All references to Holuhraun in this study refer to the older Holuhraun eruptions, unless otherwise stated. The samples from Askja central volcano comprise two basaltic tuff sequences located on the northeast and southwest shores of Öskjuvatn lake, erupted between 3.6 and ~3.0 ka BP; basaltic tephra erupted in January 1875 (denoted 1875-J) and March 1875 (denoted 1875-M); and three small eruptions from the early 20th century (c.1910, 1921, and 1922–23). The most northerly samples were collected from the 1875 AD Nýjahraun fissure eruption, located 45–60 km north of Askja central volcano. Before performing the measurements described below, all samples were thoroughly cleaned to remove old gold and carbon coatings, and re-polished to remove analysis pits from previous ion probe measurements.

The Reykjanes Ridge samples comprise quenched basaltic glass from pillows or sheet flows, collected at radial distances of ~1100 to ~400 km from the Iceland plume centre (Murton, 1995; Murton et al., 2002).

2.1. Volatiles and light elements

Melt inclusion sulfur contents were measured alongside the major elements reported by Hartley and Thordarson (2013), using the Cameca SX-100 electron microprobe instrument at the University of Edinburgh. Precision and accuracy were monitored by repeat analyses of standards

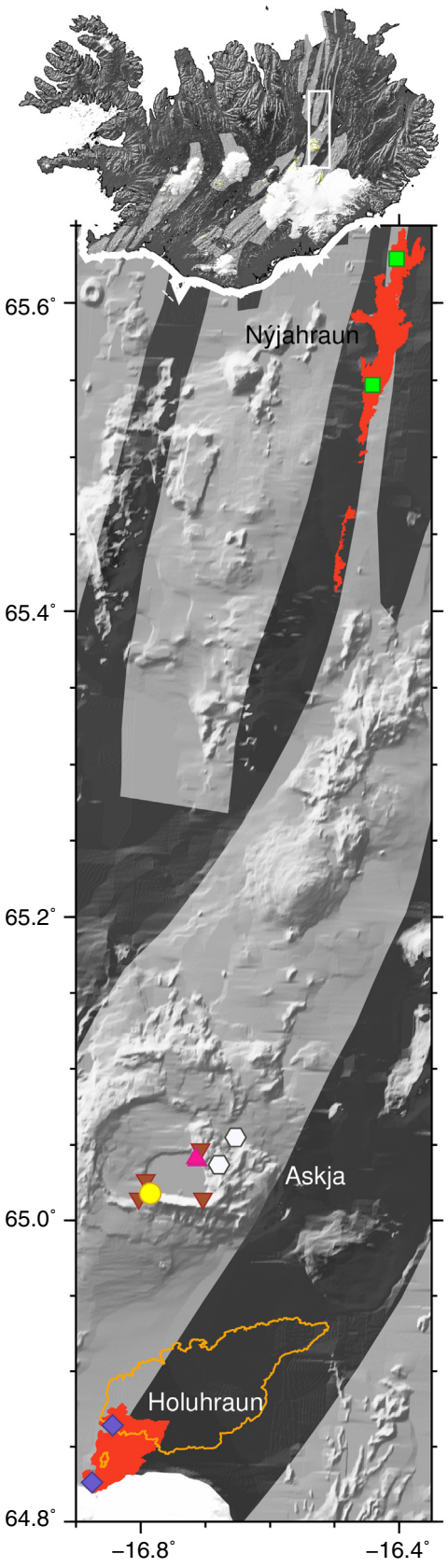

with known S concentrations, and are estimated to be better than ±3% and ±5% respectively.

Following electron microprobe analyses, a total of 165 unbreached inclusion-hosted vapour bubbles and 3 fluid inclusions from 23 different crystals were analysed by micro-Raman spectroscopy using a Horiba LabRam instrument at the University of Cambridge, following the method outlined by Hartley et al. (2014). Olivines typically host only 1–4 melt inclusions, whereas some plagioclases contain melt inclusion assemblages of 30 or more inclusions. The majority of analyzed bubbles were hosted in inclusions that were not opened for geochemical analysis. Of those inclusions exposed at the sample surface, 21 had unbreached bubbles that were analysed by Raman spectroscopy, and two had breached bubbles that could not be analysed. It is possible that some of the exposed inclusions hosted bubbles that were completely removed during sample preparation prior to visual inspection.

Melt inclusion and bubble lengths and widths were measured from high-resolution photomicrographs taken using Zeiss AxioVision software. Inclusion and bubble volumes were then calculated assuming a regular ellipsoidal shape and that depth was equal to the shorter of the measured dimensions. The melt inclusions range from 5 to 300 μm in their longest dimension (average 54 μm). Bubbles had diameters of 1–60 μm (average 9 μm). In all but 13 of the bubble-bearing melt inclusions, the bubble occupied <5% of the inclusion volume (average 1.2 vol.%). Of the remaining inclusions, 12 had bubbles occupying between 5 and 13 vol.% of the inclusion, and one bubble comprised 42 vol.% of its host inclusion.

The presence of CO_2 in fluid bubbles is verified by the presence of Fermi diad peaks at ~1285 cm^{-1} and ~1380 cm^{-1} in the Raman spectum. The Fermi diad spacing, Δ, was converted to fluid density using the equation of Kawakami et al. (2003). The fluid is assumed to be pure CO_2 since we did not detect any characteristic bands corresponding to other volatile species such as H_2O, SO_2 or SO_4^{2-} in any of the Raman spectra.

Following Raman analyses, volatile (CO_2, H_2O, F, Cl) and light element (B, Li) concentrations in 74 melt inclusions and 31 matrix glasses were determined by secondary ion mass spectrometry (SIMS) using the Cameca ims-4f instrument at the Edinburgh Ion Microprobe Facility. CO_2 was measured first, with the instrument configured to a high mass resolution to resolve any interference by $^{24}Mg^{2+}$ on the $^{12}C^{+}$ peak. The remaining elements were

Fig. 1. Map of North Iceland, with fissure swarms shown in light grey. Filled symbols show the locations of samples used in this study: green squares, Nýjahraun; pink triangle, NE tuff; yellow circle, SW tuff; white hexagons, basaltic scoria from January 1875; brown inverted triangles, early 20th century eruptions; blue diamonds, old Holuhraun eruptions. The Nýjahraun and old Holuhraun lava flow fields are shown in red. The 2014 Holuhraun lava flow field is outlined in orange. (For interpretation of the references to color in this figure legend, the reader is referred to the web version of this article.)

then measured in the same spots during a second round of analyses with the instrument configured to lower mass resolution. Precision and accuracy for CO_2 and H_2O were monitored by repeat analyses of standards with known compositions (Shishkina et al., 2010) and were ±10.8% and ±10% for CO_2, and ±8% and ±8% for H_2O. Precision and accuracy for light elements were monitored by repeat analyses of glass standards NIST-SRM610, GSA-1G, GSD-1G, and BCR2-G. Accuracy was typically better than ±5% for Li, ±6% for B, and ±20% for F and Cl. Average precision was as follows: Li, ±3%; B, ±4%; F, ±11%; Cl, ±22%. All errors are 2σ.

Boron and lithium concentrations were measured in 65 basalt glasses from the Reykjanes Ridge in a separate session under similar operating conditions. Each sample was measured twice or three times, and the results averaged.

2.2. Boron isotopes

Boron isotopic ratios in North Iceland samples were measured for 63 melt inclusions and 37 matrix glasses using the Cameca ims-1270 instrument at the Edinburgh Ion Microprobe Facility. Samples were re-polished to remove old analysis pits. Boron isotope analyses were then made in the same locations as the volatile and light elements, with the exeption of 6 glasses that were not previously analysed. Five silicate glass standards with known boron isotopic ratios (GSD-1G, StHs6/80-G, GOR128-G, GOR132-G and BCR2-G) were measured at regular intervals during the session to assess precision and accuracy. Standard glass GSA-1G was mounted alongside the unknowns and analysed at regular intervals to monitor and correct for instrumental drift. The mean internal precision was 0.95 ± 0.47‰ (2SD) across the five glass standards. The external precision, or reproducibility, is estimated at 1.49‰ based on $n = 19$ measurements on GSD-1G. The propagated uncertainty on the correction for instrumental mass fractionation is equivalent to ±0.28‰. The reported total analytical uncertainties on the North Iceland unknowns take into account the internal precision (uncertainty on an individual analysis), the external precision, and the propagated uncertainty on the instrumental mass fractionation correction, and range from 1.7 to 6.1‰ (2SD; average 3.1‰). Full details of the error propagation calculation are provided as supplementary information.

Boron isotope ratios in 50 Reykjanes Ridge glasses were measured in a separate analytical session using similar operating conditions, divided into three sub-sessions based on minor differences in beam conditions. Precision and accuracy were monitored using the same set of standard glasses, with the exception of GOR132-G. Standard glass BCR-2G was mounted alongside the unknowns and measured at regular intervals to monitor instrumental drift, which was negligible. The mean internal precision was 0.95 ± 0.85‰ (2SD) across the four glass standards and three sessions. The external precision was assessed through repeat measurements on GSD-1G in each subsession, and is 1.1‰ or better. Propagated uncertainty on the correction for instrumental mass fractionation is equivalent to 0.5, 0.4 and 0.2‰ for sub-sessions 1, 2, and 3. Each of the Reykjanes Ridge unknowns was measured at least five times. The total analytical uncertainty on individual measurements ranged from 2.1 to 7.9‰ (2SD; average 3.2‰). We have reported the $\delta^{11}B$ values for the Reykjanes Ridge glasses as the average of n measurements, and uncertainties are reported as 2 standard error of the mean which ranges from 0.7 to 3.4‰ (average 1.5‰). Further details about the analytical methods and data processing are provided as supplementary material.

3. RESULTS

3.1. Summary of major elements and post-entrapment crystallization corrections

The major element compositions measured in glasses and melt inclusions from the Askja NE and SW tuff sequences, Nýjahraun and Holuhraun, are described in detail by Hartley and Thordarson (2013). The melt inclusion compositions were previously argued to be close to equilibrium with their host minerals, and minimally modified by post-entrapment crystallization (PEC). However, applying an empirical PEC correction similar to that of Neave et al. (2017) reveals that some plagioclase-hosted melt inclusions did experience substantial PEC prior to quenching. We added equilibrium plagioclase incrementally back into the inclusion until its Al_2O_3, FeO and MgO contents match those of Icelandic tholeiitic glasses. Following this procedure, 58 out of 91 inclusions had Kd^{pl-liq}_{Ab-An} within the range 0.27 ± 0.11 appropriate for plagioclase-melt equilibrium above ⩾1050 °C (Putirka, 2008). Thirty inclusions had Kd^{pl-liq}_{Ab-An} lower than the equilibrium range, and these were all hosted in An > 86 plagioclase. Applying any further PEC correction to these inclusions in order to satisfy the equilibrium criterion results in unrealistically high Al_2O_3 compared with Icelandic tholeiitic glasses (Fig. 2); similar results have been obtained for melt inclusions in high-anorthite plagioclases from the nearby Grímsvötn volcanic system (Neave et al., 2017) and the 2014–15 Holuhraun eruption (Hartley et al., 2018). Four inclusions required subtraction of equilibrium plagioclase to satisfy the equilibrium criterion. The average PEC correction for inclusions from the Askja NE and SW tuff cones was 4% (range 0–18%), and for Holuhraun the average PEC correction was 8% (range 4–15%). Olivine-hosted melt inclusions were corrected for PEC by adding equilibrium olivine back to the inclusion until a Kd^{ol-liq}_{Fe-Mg} of 0.30 (Roeder and Emslie, 1970) was reached. The mean PEC correction for inclusions from Nýjahraun was 1.7% (range 0.0–2.5%), and for Holuhraun the average correction was 2.1% (range 0.0–6.0%).

Corrected major element compositions of melt inclusions are summarized in Fig. 2. Following PEC correction, the most primitive melt inclusions in the sample suite contain up to 9.3 wt.% MgO (Fig. 2) and are hosted in plagioclases from Holuhraun. The most evolved melt inclusions from each sample have compositions that are comparable with their carrier liquids, represented by the matrix glass.

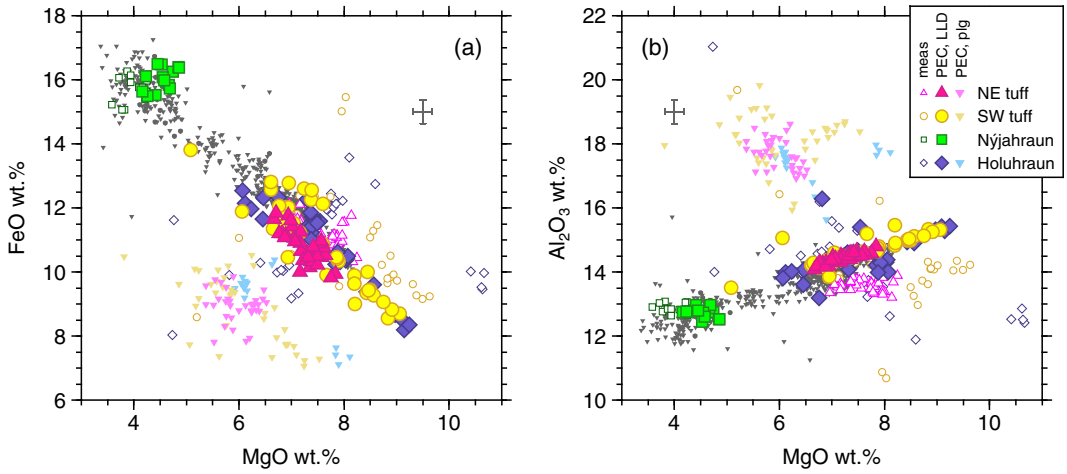

Fig. 2. Major element compositions of melt inclusions and glasses from North Iceland. Error bars are 2σ. Small grey inverted triangles show matrix glasses from the Askja and Bárðarbunga volcanic systems. Coloured open symbols show raw (uncorrected) melt inclusion compositions. Large filled symbols show melt inclusions corrected for post-entrapment crystallization. Plagioclase-hosted inclusions were corrected by adding equilibrium plagioclase until their MgO-FeO-Al_2O_3 systematics matched those of Icelandic tholeiitic glasses; olivine-hosted inclusions were corrected by adding equilibrium olivine until their compositions met the equilibrium criterion $Kd_{Fe-Mg}^{ol-liq} = 0.30 \pm 0.03$. Small pale inverted triangles show plagioclase-hosted melt inclusions corrected to be in equilibrium with their host crystal, which results in unrealistically high Al_2O_3 contents. (For interpretation of the references to color in this figure legend, the reader is referred to the web version of this article.)

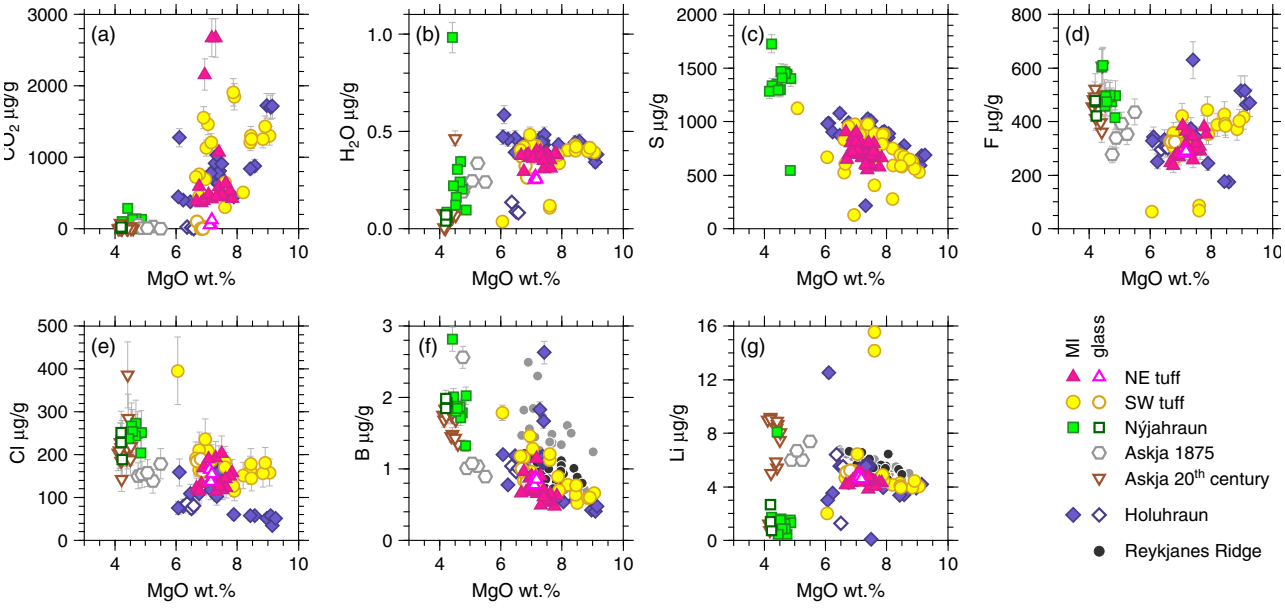

Fig. 3. Volatile and light element concentrations in melt inclusions and matrix glasses from North Iceland. Melt inclusions are shown in solid symbols, and matrix glasses in open symbols. Error bars are 2σ and in many cases are smaller than the symbol size. Black circles show Reykjanes Ridge glasses collected at radial distance >620 km from the Iceland plume centre, and filtered to exclude samples that could possibly have gained B through assimilation of a B-rich contaminant (see Section 4.3 for details); all other Reykjanes Ridge glasses are shown as grey circles.

Volatile and light element contents of melt inclusions were corrected for PEC assuming that they are perfectly incompatible in olivine and plagioclase. Melt inclusion trace element contents were corrected for PEC using partition coefficents from O'Neill and Jenner (2012). Boron and oxygen isotopes are not significantly fractionated during basalt crystallization (Eiler, 2001; Marschall et al., 2017), so no PEC correction is required.

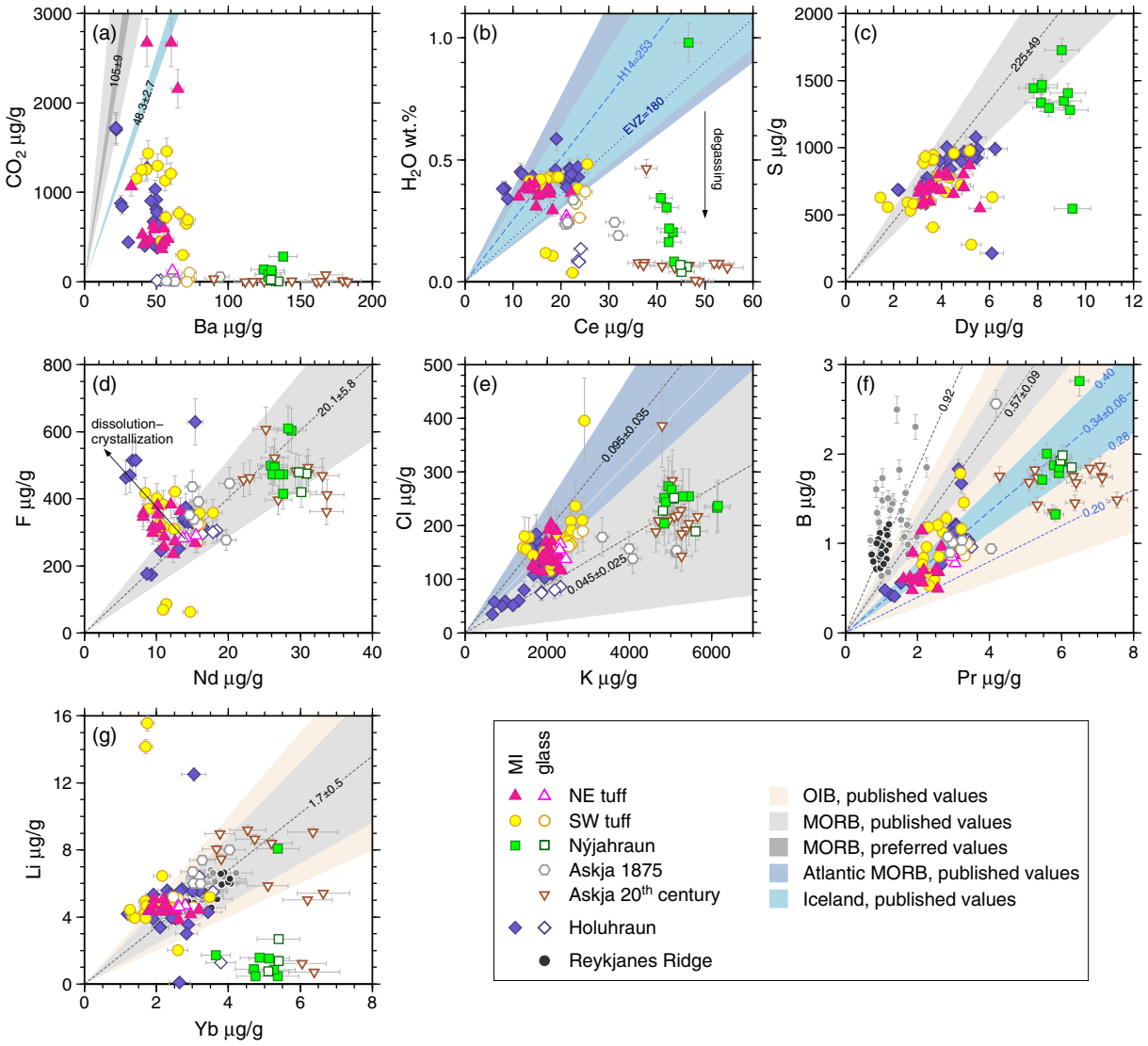

Fig. 4. Volatile-trace element systematics in melt inclusions and matrix glasses from North Iceland. Error bars are 2σ. The B and Li contents of Reykjanes Ridge glasses are shown in panels (f) and (g). Black circles show Reykjanes Ridge glasses collected at radial distance >620 km from the Iceland plume centre, and filtered to exclude samples that could possibly have gained B through assimilation of a B-rich contaminant (see Section 4.3 for details); all other Reykjanes Ridge glasses are shown as grey circles. The shaded regions show published volatile-trace element ratios for different mantle reservoirs. MORB: CO_2/Ba from Michael et al. (2015), H_2O/Ce from Michael (1995), S/Dy from Saal et al. (2002), F/Nd from Workman et al. (2006), Cl/K from Michael and Cornell (1998), B/Pr and Li/Yb from Marschall et al. (2017). OIB: B/Pr range for Hawaii melt inclusions from Edmonds (2015); Li/Yb range from Ryan and Langmuir (1987), Edmonds (2015). Iceland: CO_2/Ba from Hauri et al. (2018), H_2O/Ce from Hartley et al. (2015) and Bali et al. (2018); B/Pr from this study.

3.2. Volatiles and light elements

New volatile and light element analyses for our North Iceland and Reykjanes Ridge samples are summarized in Fig. 3, and plotted against similarly incompatible trace elements in Fig. 4.

3.2.1. Carbon dioxide

The CO_2 contents of matrix glasses and the evolved Nýjahraun melt inclusions are low (50–284 µg/g), and in some cases are lower than the detection limit of ~24 µg/g (Fig. 3a). The more primitive melt inclusions (>6 wt.% MgO) have a wide range of CO_2 contents (365–2670 µg/g), but most inclusions have CO_2 contents close to the mean values of 806 µg/g for the Askja NE tuff, 1036 µg/g for the SW tuff, and 867 µg/g for Holuhraun.

We detected no Fermi diad peaks in the Raman spectra of 143 out of 165 inclusion-hosted bubbles, suggesting that they contain $\ll$0.04 g/cm^3 CO_2 (Hartley et al., 2014) and make no significant contribution to the total melt inclusion CO_2 content (e.g. Steele-MacInnis et al., 2011). These apparently empty bubbles typically occupy <3 vol.% of their host inclusion (Fig. S2.1). They are most likely true shrinkage bubbles, formed due to differential thermal con-

traction of the host olivine and silicate melt upon quenching, and with negligible diffusive transfer of CO_2 from the silicate melt into the vapour phase. CO_2 fluid was detected in 22 inclusion-hosted bubbles and one fluid inclusion. These were hosted in one olivine crystal from Holuhraun (one bubble, one fluid inclusion); two plagioclases from the NE tuff (three bubbles); and four plagioclases from the SW tuff (17 bubbles).

Fluid densities for the 22 CO_2-bearing inclusion-hosted bubbles were converted to CO_2 contents in μg/g on a per-inclusion basis, after estimating the volumes of the bubble and the glass, following the mass-balance approach of Steele-MacInnis et al. (2011). We assumed a melt density of 2750 kg/m^3 for the mass balance calculations. The calculated bubble CO_2 contents range from 86 to >11,000 μg/g (average 1860 μg/g). For CO_2-bearing bubbles, there is a strong positive correlation between bubble CO_2 content and the bubble volume fraction of the melt inclusion.

We find no differences in the glass CO_2 contents of bubble-bearing versus bubble-free inclusions. Given that 143 out of 165 inclusion-hosted bubbles contain no detectable CO_2 and are most probably true shrinkage bubbles, we can assume that melt inclusion glasses typically record the total melt inclusion CO_2 content at quenching. For three of our melt inclusions (two olivine-hosted inclusions from Holuhraun and one plagioclase-hosted inclusion from the SW tuff) it is necessary to add the glass and bubble CO_2 contents to yield the total inclusion CO_2 content. These inclusions have total CO_2 contents of 880–1980 μg/g, within the ranges of measured glass CO_2 contents in the same samples. The percentage of CO_2 sequestered into the fluid phase were 5% and 13% for the two Holuhraun inclusions, and 73% for the plagioclase-hosted inclusion from the SW tuff.

3.2.2. Water

Melt inclusion H_2O contents for Holuhraun and the Askja tuff sequences cluster around 0.39 ± 0.08 wt.%, with no statistically significant differences between eruptions and no correlation of H_2O with MgO (Fig. 3b). Most Nýjahraun melt inclusions lie between the most H_2O-rich and H_2O-poor matrix glasses, and the positive correlation of H_2O with MgO suggests that these inclusions were trapped as H_2O was degassing. A single melt inclusion containing 0.98 wt.% H_2O may record the undegassed pre-eruptive melt H_2O content.

3.2.3. Sulfur, fluorine, chlorine

Melt inclusion sulfur contents are variable (typically 400–1730 μg/g; Fig. 3c), and are negatively correlated with MgO (R^2=0.63).

The North Iceland matrix glasses contain an average 400 ± 180 (2SD) μg/g fluorine (Fig. 3d). They have similar F contents to the evolved melt inclusions, suggesting that there was minimal F degassing before the matrix glasses were quenched. More primitive melt inclusions contain 60–620 μg/g F. In olivine-hosted melt inclusions, F is negatively correlated with MgO (Fig. S2.2), but this correlation is absent for plagioclase-hosted melt inclusions (Fig. S2.3).

Chlorine in matrix glasses ranges from 75 to 380 μg/g (Fig. 3e). Holuhraun melt inclusions contain 60–185 μg/g Cl, and Cl is negatively correlated with MgO. Melt inclusions from the Askja tuff cones have slightly higher Cl contents of 110–395 μg/g, and are more Cl-rich at any given MgO content than inclusions from Holuhraun.

3.2.4. Boron, lithium

Both B and Li are broadly negatively correlated with MgO (Fig. 3f,g), consistent with a dominant fractional crystallization control on the concentrations of these incompatible trace elements. All the glasses and melt inclusions measured in this study contain between 0.3 and 2.9 μg/g B, similar to the B contents measured in global MORB datasets (Marschall et al., 2017). Several Reykjanes glasses, and a small number of melt inclusions, have slightly higher [B] than the main population of North Iceland melt inclusions. Two Reykjanes Ridge glasses located <500 km from the putative Iceland plume centre have slightly higher [B] than most Reykjanes Ridge samples; however, the apparent increase in the mean [B] of Reykjanes Ridge samples approaching Iceland is not significant on the lengthscale of the whole dataset (Fig. 5b).

Askja and Holuhruan matrix glasses contain 0.1–9.2 μg/g Li (Fig. 3g). Reykjanes Ridge glasses contain 3.7–6.7 μg/g Li, and there is no systematic along-ridge variability in Li content (Fig. 5a). They are compositionally indistinguishable from the main population of North Iceland melt inclusions. A small number of melt inclusions have low Li contents down to 0.1 μg/g, and two inclusions have anomalously high Li contents up to 16 μg/g.

3.3. Boron and oxygen isotopes

Boron isotopic compositions of the North Iceland melt inclusions range from −20.7 to +0.6‰. Across the whole dataset the modal $\delta^{11}B = -5.9$‰, where 'modal' refers to the peak in the probability distribution, here and throughout the text. The modal $\delta^{11}B$ values are −6.1 to −6.4‰ for Holuhraun and the Askja tuff sequences, and −4.9‰ for Nýjahraun (Fig. S2.7). The North Iceland glasses have $\delta^{11}B$ between −10.6 and −4.0‰, and the modal $\delta^{11}B$ value is −5.6‰ (Fig. S2.7). Reykjanes Ridge glasses have $\delta^{11}B$ between −7.9 and −3.6‰. Their modal $\delta^{11}B$ is $-6.1 \pm (2SD = 2.0‰,\ 2SE = 0.5‰,\ n = 50)$. There is no along-ridge variability in $\delta^{11}B$ (Fig. 5c) and there is no correlation between [B] and $\delta^{11}B$. For both North Iceland and Reykjanes Ridge samples, the modal $\delta^{11}B$ values are higher than the −7.1 ± 0.9‰ (mean of six ridge segments, 2SD) proposed for uncontaminated MORB (Marschall et al., 2017). However, all the North Iceland samples contain melt inclusions that are isotopically lighter than the proposed MORB range. Some inclusions from Holuhraun and the Askja tuff sequences have $\delta^{11}B$ within the range −11.3 ± 3.8‰ measured in primitive olivine-hosted melt inclusions from the Western Volcanic Zone and Reykjanes Peninsula (Gurenko and Chaussidon, 1997).

The North Iceland melt inclusions show no statistically significant correlations between $\delta^{11}B$ and indices of melt

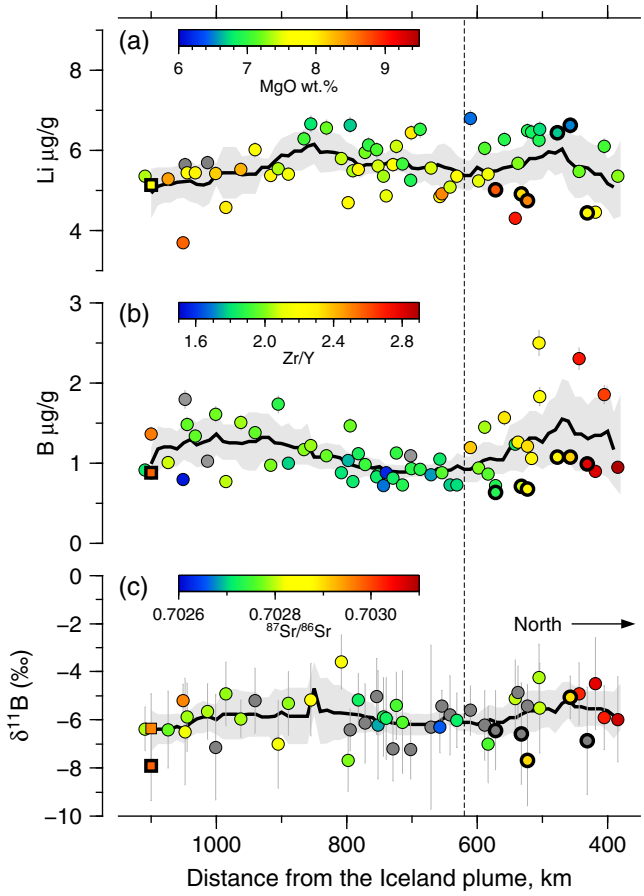

Fig. 5. Along-ridge variation in [Li], [B] and $\delta^{11}B$ of Reykjanes Ridge glasses. Data are plotted as a function of radial distance from the Iceland plume centre and coloured according to (a) MgO content, (b) Zr/Y and (c) $^{87}Sr/^{86}Sr$ of the sample glasses. Samples with bold outlines have B/Pr within the expected MORB range of 0.57 ± 0.09. Square symbols denote samples from enriched seamount 14D. The increases in Zr/Y and $^{87}Sr/^{86}Sr$ at radial distances <620 km indicate the influence of an enriched mantle compoment associated with the Iceland plume. Samples at radial distances >620 km are not influenced by the enriched plume component and sample ambient Reykjanes Ridge mantle. Black lines show the running average composition calculated using a boxcar filter with a bandwidth of 100 km; the grey shaded area shows the error envelope (2SE) of the filtered data. Two samples at radial distances ~500 km appear to have high [B], but the increase in mean [B] approaching Iceland is not significant on the lengthscale of the whole dataset. There is no systematic along-ridge variability in [Li] or $\delta^{11}B$. Major element data from Shorttle et al. (2015); trace element data from Novella et al. (2020); isotope data from Murton et al. (2002) and Thirlwall et al. (2004).

evolution. However, if literature and Reykjanes Ridge data are included, the lowest $\delta^{11}B$ values appear to be associated with the most primitive melt and host mineral compositions (Fig. S2.9). For olivine-hosted melt inclusions, $\delta^{11}B$ and MgO are negatively correlated with $R^2 = 0.60$ (Fig. 6a). Plagioclase-hosted inclusions have widely variable $\delta^{11}B$ at near-constant MgO or B content (Fig. S2.9): for example, melt inclusions from the Askja SW tuff containing 6.0–9.0 wt.% MgO have $\delta^{11}B$ ranging from −20.7 to −2.6‰.

Oxygen isotopic compositions of the North Iceland melt inclusions and glasses are summarized in Fig. 6b. The strong positive correlation between $\delta^{18}O$ and MgO wt.% has been interpreted as evidence of assimilation of a low-$\delta^{18}O$ basaltic crustal component (Hartley et al., 2013). We find no statistically significant correlation between $\delta^{11}B$ and $\delta^{18}O$ in the North Iceland dataset (Fig. S2.8).

4. DISCUSSION

4.1. Melt inclusion trapping pressures

The boron contents and $\delta^{11}B$ signatures of basaltic magmas are potentially highly sensitive to small degrees of assimilation of hydrothermally altered crustal material. The few published measurements of [B] and $\delta^{11}B$ in Icelandic upper crustal materials suggest that they have high B contents of ~3–12 µg/g, and heterogeneous boron isotopic compositions between −18.3 and −4.4‰ (Raffone et al., 2008; Raffone et al., 2010). Thus, even small degrees of upper crustal assimilation could exert strong influence on the boron contents and $\delta^{11}B$ of ascending basaltic magmas, particularly when the concentration and isotopic contrasts between melt and assimilant are high. In contrast, the Icelandic lower crust is constructed through repeated melt

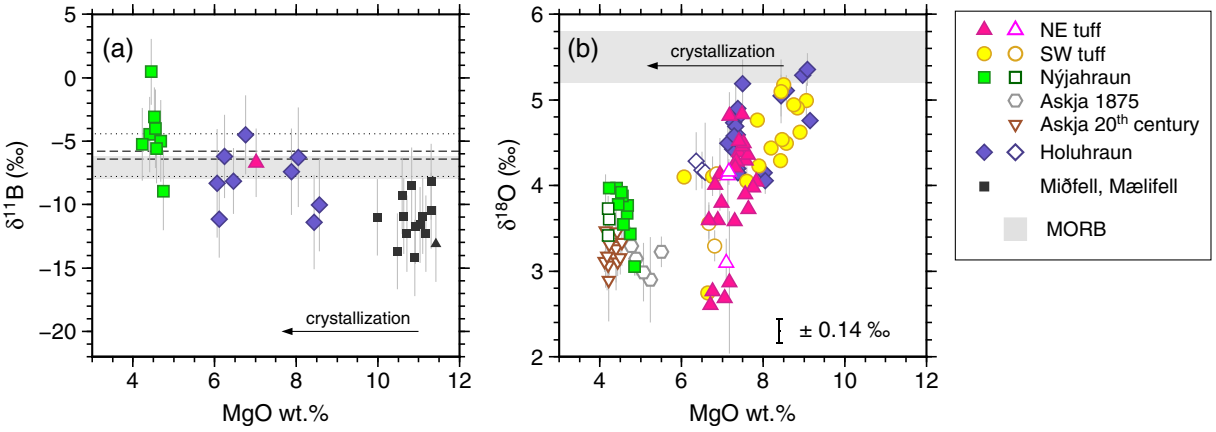

Fig. 6. (a) Boron isotopic compositions of olivine-hosted melt inclusions from Iceland. Miðfell data are from Gurenko and Chaussidon (1997). (b) Oxygen isotopic compositions of North Iceland melt inclusions and glasses vs MgO, an index of melt evolution. Oxygen isotope data are from Hartley et al. (2013). Error bars are 2σ. Shaded grey bars indicate δ^{11}B and δ^{18}O for pristine MORB glasses (Chaussidon and Marty, 1995; Marschall et al., 2017). The modal boron isotopic composition of Reykjanes Ridge glasses is −6.1‰; dashed lines in (a) indicate the 2SE range of ±0.3 and dotted lines indicate the 2SD of ±1.7‰. High-temperature crystallization is not expected to fractionate boron or oxygen isotopes, therefore the observed trends can only be generated through assimilation processes.

injections (e.g. Greenfield and White, 2015, and references therein), thus there will be little compositional or isotopic difference between melts intruded into the lower crust and their surrounding material. Melt inclusions trapped during crystallization in the lower crust are therefore expected to record the least modified boron isotopic compositions, since their carrier melts will have had minimal opportunity to assimilate B-rich, isotopically distinctive altered upper crustal material.

Melt inclusion and glass equilibration pressures can be estimated using the position of the olivine-plagioclase-augite-melt (OPAM) thermal minimum, provided that the melt is saturated in all three phases. All the North Iceland samples contain olivine, clinopyroxene and plagioclase crystals, although it is not possible to visually assess whether glassy melt inclusions were trapped from a three phase-saturated melt. We calculated OPAM equilibration pressures for the North Iceland melt inclusions and glasses using the Yang et al. (1996) parameterization of the OPAM barometer, following the method of Hartley et al. (2018). The calculation is performed in two steps. First, Eqs. (1)–(3) of Yang et al. (1996) are solved iteratively at 1 MPa intervals between −0.5 and 1.5 GPa. The predicted cation mole fractions of Mg, Ca and Al are then compared with the input melt composition, and the best fitting model equilibration pressure is chosen to minimise the χ^2 misfit between measured and predicted melt compositions. Second, the quality of fit between the predicted and measured melt compositions is assessed by using the χ^2 vs. pressure distribution to define a significance criterion P_F, whereby only samples that pass the filter $P_F \geqslant 0.8$ are considered to be three phase-saturated (Hartley et al., 2018). The high threshold of the P_F filter ensures that one- or two-phase-saturated melts that could yield erroneously high OPAM pressures are effectively screened out and not considered further.

We calculated OPAM equilibration pressures for the North Iceland melt inclusions using both measured and PEC-corrected compositions. Only 20 out of 121 measured melt inclusion compositions met the $P_F \geqslant 0.8$ criterion, rising to 53 inclusions when PEC-corrected compositions are considered. The returned equilibration pressures are summarized in Fig. 7. The highest pressure of 0.57 GPa was returned for a plagioclase-hosted melt inclusion from the SW tuff. Assuming a mean crustal density of 2860 kg/m^3, this corresponds to a depth of 20.5 km. The crustal thicknesss is 30–35 km in the Askja region (Darbyshire et al., 2000), so our deepest-trapped melt inclusion records crystallization in the lower crust (e.g. Winpenny and Maclennan, 2011). The modal equilibration pressures are 0.36 GPa (12.9 km) for Holuhraun, 0.31 GPa (11.1 km) for the NE tuff, and 0.47 GPa (16.6 km) for the SW tuff. The lowest equilibration pressures of 0.10–0.15 GPa (3.6–5.3 km) were for olivine-hosted inclusions from Holuhraun. No melt inclusions from Nýjahraun passed the $P_F \geqslant 0.8$ criterion.

There appears to be a broad correlation between melt inclusion composition and trapping pressure, with more primitive inclusions returning deeper trapping pressures. However, it is difficult to assess the significance of this relationship given the ±0.13 GPa uncertainty of the OPAM barometer. The median δ^{11}B decreases with decreasing pressure (Fig. 7b), although the magnitude of this decrease is smaller than analytical uncertainty on individual measurements. The δ^{11}B values are widely scattered across the entire crystallization interval. To characterise the dispersion of δ^{11}B we use the median absolute deviation, σ^*, which is not sensitive to outliers:

$$\sigma^* = k\mathrm{med}(|x_i - \mathrm{med}(x_j)|) \quad (1)$$

where $k \approx 1.48$ for normally distributed data, and med(x_i) refers to the median of ordered dataset x_i. We assume that,

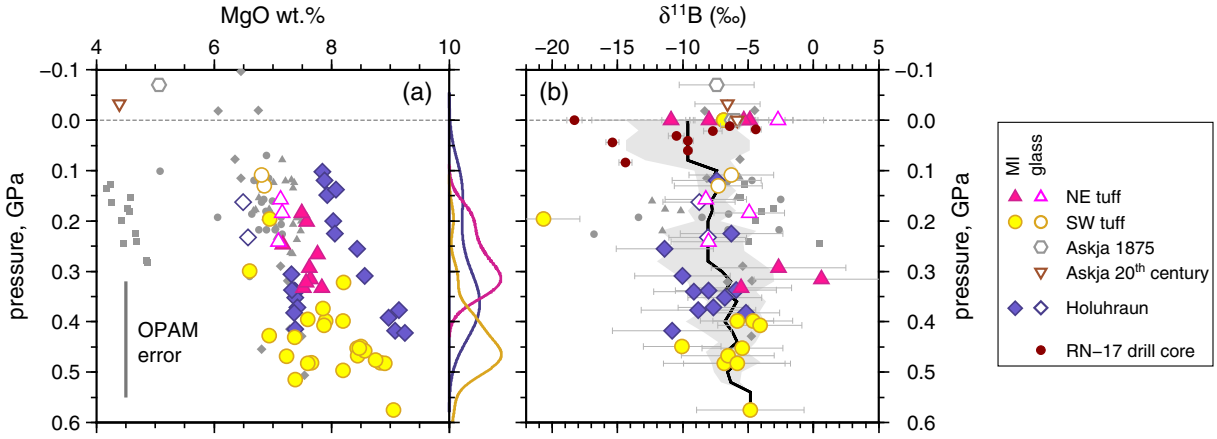

Fig. 7. Application of the Yang et al. (1996) OPAM barometer to melt inclusions and glasses from North Iceland. Large coloured symbols show PEC-corrected melt inclusion compositions where the returned probability of fit P_F is greater than 0.8. Small grey symbols show melt inclusion compositions where $P_F < 0.8$. Kernel density estimates to the right of plot (a) show the relative probability of equilibration pressures for melt inclusion compositions with $P_F \geqslant 0.8$, coloured according to the source eruption. Dark red circles in (b) show boron isotopic compositions of whole-rock samples from drill core RN-17, Reykjanes Peninsula (Raffone et al., 2008), where the sampled depth in the core is converted to pressure assuming an upper crustal density of 2860 kg/m^3. The black line shows the running median δ^{11}B as a function of depth, calculated using a boxcar filter with a bandwidth of 0.5 GPa; the grey shaded area shows the median absolute deviation. (For interpretation of the references to color in this figure legend, the reader is referred to the web version of this article.)

at any given pressure, the dispersion in δ^{11}B is normally distributed. The median absolute deviation suggests that the variability in δ^{11}B generally increases with decreasing pressure, and is greatest in the uppermost 0.1 GPa (3.5 km) of the crust (Fig. 7b).

4.2. Volatile-trace element systematics: primary versus modified signatures

Fig. 4 shows melt inclusion volatile concentrations each plotted against a similarly incompatible trace element. These element pairs are expected to exhibit similar geochemical behaviour during the crystallization of volatile-undersaturated melts (e.g. Michael, 1995; Dixon and Clague, 2001; Saal et al., 2002; Michael and Graham, 2013; Rosenthal et al., 2015).

The average CO_2/Ba recorded in melt inclusion suites is controlled by mixing between variably degassed melts, such that the maximum CO_2/Ba in a melt inclusion dataset may not reflect the mantle source CO_2/Ba (Matthews et al., 2017). Published estimates of CO_2/Ba in nominally undegassed Icelandic melt inclusions range from 48 (Hauri et al., 2018) and 80–90 (Hartley et al., 2014; Neave et al., 2014) up to 396 (Miller et al., 2019). Only four of our North Iceland melt inclusions could reflect undegassed or minimally degassed melts: three inclusions from Holuhraun with CO_2/Ba of 77–79 and one inclusion from the Askja NE tuff with CO_2/Ba = 62. All the remaining melt inclusions have CO_2/Ba<44, and the negative correlation between CO_2 and Ba (Fig. 4a) is consistent with crystallization occurring concurrently with CO_2 degassing. We used the major element compositions and total CO_2 contents of melt inclusions to calculate volatile saturation pressures following the method of Shishkina et al. (2014). Calculated volatile saturation pressures fall between 0.37 and 0.02 GPa, and are on average 0.18 GPa lower than the equivalent OPAM pressure (Fig. S2.11). This discrepancy, combined with the number of inclusions with apparently CO_2-free bubbles in our sample set, suggests that many of the inclusions have been affected by decrepitation. This occurs when the internal pressure of the inclusion exceeds the tensile strength of the host mineral resulting in loss of CO_2 vapour (Maclennan, 2017). The calculated volatile saturation pressures thus provide a minimum estimate of the pressure at which the inclusion was trapped.

The North Iceland melt inclusions have H_2O/Ce, S/Dy, F/Nd, Cl/K and Li/Yb values that fall broadly within the expected ranges for undegassed and unmodified primary melts of MORB or OIB affinity (Fig. 4). Reykjanes Ridge glasses have Li/Yb values that are indistinguishable from the North Iceland samples. The mean H_2O/Ce across our melt inclusion dataset is 219, and most of the North Iceland inclusions fall within the expected range for Icelandic melts (Hartley et al., 2015; Bali et al., 2018), suggesting that there has been minimal post-entrapment modification of melt inclusion H_2O contents through diffusive H^+ exchange with their carrier melts. A number of plagioclase-hosted melt inlusions have significantly higher F/Nd than the expected MORB range, which is consistent with a dissolution-crystallization process resulting in the trapping of an Al- and F-rich boundary layer (Neave et al., 2017). The high-Li, high-Li/Yb signatures in two melt inclusions from the SW tuff are not associated with enrichment in any other incompatible or volatile element, and could reflect trapping of Li-oversaturated melt pockets during crystallization (e.g. Hartley et al., 2018). Finally, several low H_2O/Ce and Li/Yb melt inclusions from Nýjahraun are likely to have been trapped during late-stage crystallization of a partially H_2O- and Li-degassed melt. Further information on H_2O/Ce, S/

Dy, F/Nd, Cl/K and Li/Yb systematics is provided as supplementary material.

The North Iceland melt inclusions have B/Pr between 0.17 and 0.58, and mostly lie within the range 0.34 ± 0.06 (Fig. 4f). All but six plagioclase-hosted inclusions have lower B/Pr than the global MORB average of 0.57 ± 0.09 (Marschall et al., 2017). Reykjanes Ridge glasses have widely variable B/Pr (0.4–1.9; Pr data from Novella et al. (2020)), and most have higher B/Pr than the published global MORB range (Fig. 4f).

4.3. Boron content and isotopic composition of Reykjanes Ridge mantle

Reykjanes Ridge basalts show well-documented along-ridge shifts in incompatible trace element concentrations, lithophile and noble gas isotopic ratios, and fO_2 north of 61 °N (Hart et al., 1983; Schilling et al., 1983; Murton et al., 2002; Shorttle et al., 2015), indicating that the presence of an enriched, plume-influenced mantle component beneath the northern ridge segment is likely. Glasses collected at radial distances >620 km from the putative plume centre do not show this distinctive enrichment, but sample ambient Reykjanes Ridge mantle. To elucidate the boron isotopic composition of this mantle component, we have filtered the Reykjanes Ridge sample set to consider only those collected at radial distance >620 km. We also exclude two samples from enriched seamount 14D located 1100 km from the plume centre (Murton et al., 2002). None of the filtered samples have B/Pr within the expected MORB range: of the seven samples with B/Pr of 0.57 ± 0.09, six are proximal to Iceland and the seventh is from the enriched seamount (Fig. S2.12).

The filtered Reykjanes Ridge glasses have remarkably constant Pr contents of 1.0 ± 0.3 μg/g (2SD) (Fig. S2.13). Their boron contents range between 0.7 to 1.8 μg/g (mean 1.1 ± 0.6 2SD), but show no systematic variation with distance from Iceland (Fig. 5b). The modal $\delta^{11}B$ value is −6.1‰ (2SD = 1.7‰, 2SE = 0.3‰, $n = 31$) and there is no correlation between [B] and $\delta^{11}B$. A very weak negative correlation between B/Pr and $\delta^{11}B$ with R^2=0.19 is not statistically significant within uncertainty.

To maximise the likelihood that we are considering only samples that have not gained boron through assimilation of seawater, brines or altered oceanic crust, we apply further stringent filtering to exclude any samples with [B] >1.25 μg/g or B/Pr > 1.4. The remaining samples contain on average 0.92 ± 0.29 (2SD) μg/g B and 1.0 ± 0.2 (2SD) μg/g Pr; their average B/Pr is 0.92 (2SD = 0.29, 2SE = 0.06, $n = 27$), and the modal $\delta^{11}B$ is −6.1‰ (2SD = 1.5‰, 2SE = 0.3‰, $n = 21$). We are confident that this $\delta^{11}B$ value is representative of ambient depleted Reykjanes Ridge mantle. It is slightly higher than the proposed MORB range from Marschall et al. (2017), although the two ranges overlap within uncertainty. Reykjanes Ridge melts also have higher B/Pr than has been proposed for global MORB, but are similar to basalts from the Kolbeinsey Ridge, north of Iceland, which have mean B/Pr = 0.86 (Marschall et al., 2017). Both the high B/Pr and high $\delta^{11}B$ signatures of Reykjanes Ridge basalts appear to be intrinsic to the Reykjanes Ridge mantle source.

We used a simple non-modal batch melting equation and the relationships between Zr/Y and La/Y (Fig. S2.16) to show that the Reykjanes Ridge basalts likely represent 10–12% partial melts of a depleted spinel peridotite mantle. We use a bulk partition coefficient $D_{Pr} = 0.015$ for spinel peridotite (details provided as supplementary material) and a Pr content of 0.107 μg/g for depleted MORB mantle (DMM; Workman and Hart, 2005), to calculate the average boron content of Reykjanes Ridge mantle. The average [Pr] of the Reykjanes Ridge glasses, 0.87 μg/g, is reached after 11.5% partial melting of DMM. To reach an average B/Pr of 0.92 ± 0.29 after 11.5% partial melting, the mantle source should contain $\sim 0.10 \pm 0.03$ μg/g B. This suggests that Reykjanes Ridge mantle contains slightly more boron than the 0.077 ± 0.010 μg/g typical of DMM (Marschall et al., 2017).

We recover a small degree of along-ridge enrichment in [B], but $\delta^{11}B$ remains constant across the ridge segment (Fig. 5). The very limited [B] enrichment along the Reykjanes Ridge approaching Iceland suggests that the plume-derived mantle component exerts only very weak leverage on the along-ridge [B], and does not contribute substantially to the boron budget of these melts. A counterintuitive inference leading from this observation is that the enriched mantle component may be boron-poor in comparison to Reykjanes Ridge depleted mantle. This is consistent with the observation that our North Iceland melt inclusions have similar boron contents to the Reykjanes Ridge glasses (Fig. 4f), but have higher Pr contents and lower B/Pr. Given the similarly incompatible behaviour of B and Pr during mantle melting, this indicates that the North Iceland melt inclusions originate from a mantle component with lower [B] than depleted Reykjanes Ridge mantle. The absence of along-ridge variation in $\delta^{11}B$ could either reflect the low boron contribution from the enriched mantle component, or else that there is only limited boron isotopic contrast between the enriched component and ambient depleted mantle. In the next section, we explore the boron isotopic composition of the mantle beneath Iceland.

4.4. Boron content and isotopic composition of the Icelandic mantle

The modal $\delta^{11}B$ value across the North Iceland melt inclusion dataset is −5.9‰, somewhat higher than the -7.1 ± 0.9‰ range proposed for uncontaminated MORB (Marschall et al., 2017). However, the modal $\delta^{11}B$ values for melt inclusions from Holuhraun and the Askja tuff sequences lie between −6.4 and −6.1‰, within the expected MORB range. A number of inclusions from Holuhraun and the Askja tuff sequences have much lower $\delta^{11}B$ and fall within the -11.3 ± 3.8‰ that has previously been suggested to be representative of the Iceland mantle source (Gurenko and Chaussidon, 1997). A key question is therefore whether the boron isotopic signature of the Icelandic mantle is similar to, or distinct from, that of MORB.

To use the North Iceland melt incluson data to assess the boron isotopic signature of the Icelandic mantle, it is first necessary to verify that their $\delta^{11}B$ values have not been affected by pre- or post-entrapment modification. We are not aware of any published studies of boron diffusion in olivine or plagioclase, but we expect that post-entrapment modification via B diffusion through these host minerals will be negligble. Both [B] and $\delta^{11}B$ in an ascending magma could be modified prior to inclusion trapping via assimilation of altered crustal material (e.g. Chaussidon and Jambon, 1994; Chaussidon and Marty, 1995; Gurenko and Chaussidon, 1997; Rose-Koga and Sigmarsson, 2008; Brounce et al., 2012). Low $\delta^{18}O$ values measured in more evolved inclusions and glasses from North Iceland (Fig. 6b) most likely reflect progressive assimilation of hydrated low-$\delta^{18}O$ basaltic hyaloclastite in the mid- to upper crust (Hartley et al., 2013). Altered Icelandic upper crustal material has high B contents of ~3–12 μg/g, and boron isotopic compositions between −18.3 and −4.4‰ (Raffone et al., 2008; Raffone et al., 2010) (Fig. 7); therefore, the boron contents and isotopic signatures of these more evolved melt inclusions and glasses are also expected to be modified by assimilation.

A small number of our North Iceland melt inclusions have higher [B] than can be consistent with simple fractional crystallization (Fig. 2f), which indicates assimilation of a B-rich component prior to melt inclusion trapping. To exclude potentially contaminated melt inclusions from further consideration, we have filtered the melt inclusion dataset for compositions with ⩾8 wt.% MgO in order to assess the $\delta^{11}B$ of Icelandic primary melts. The MgO⩾8 wt.% melt inclusions are hosted in the most primitive olivines and plagioclases, indicating that they were trapped during the earliest stages of crystallization from melts that experienced no to minimal modification by assimilation of crustal contaminants. The effects of crustal assimilation on melt inclusion [B], $\delta^{11}B$ and $\delta^{18}O$ signatures are explored further in Section 5.

The boron isotopic compositions of primitive melt inclusions from across Iceland are shown in Fig. 8. Eleven of the North Iceland melt inclusions with available $\delta^{11}B$ measurements have ⩾8 wt.% MgO. These inclusions are hosted in some of the most primitive olivines and plagioclases, and also have high CO_2 and low S, Cl, B and Li concentrations (Fig. 2) suggesting that they are minimally degassed. These inclusions are therefore most likely to provide robust estimates of $\delta^{11}B$ for the Icelandic mantle source.

Primitive melt inclusions from Holuhraun and the Askja SW tuff have different boron isotopic signatures. Those from Holuhraun display a broad peak in the $\delta^{11}B$ probability distribution at −10.6‰ (8), which is not distinguishable from the $\delta^{11}B$ of around −11‰ for primitive WVZ melt

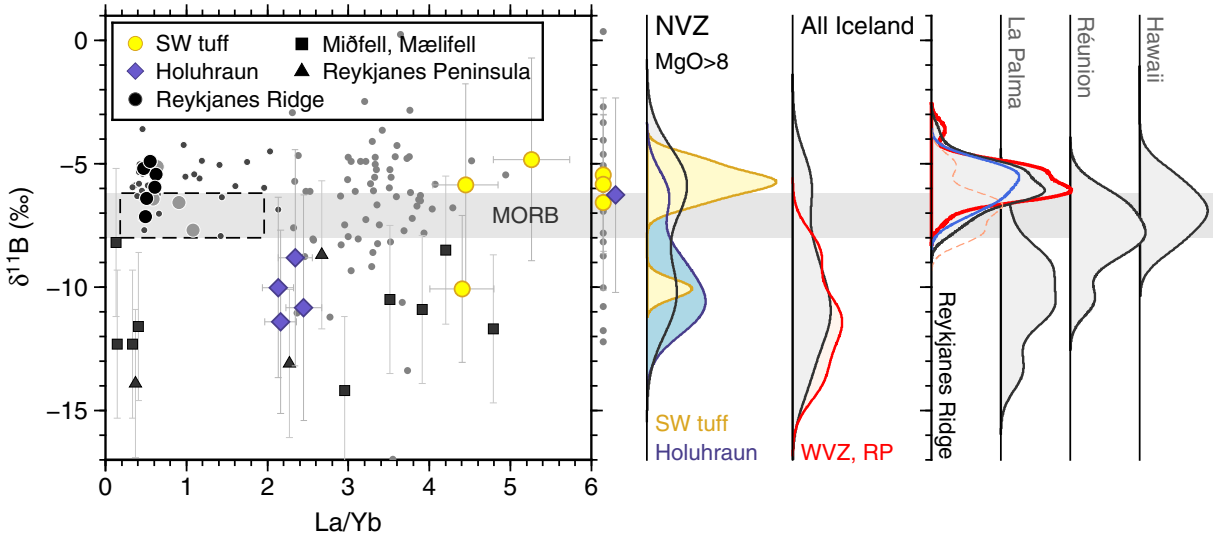

Fig. 8. Boron isotopic compositions of on-land Iceland melt inclusions and Reykjanes Ridge glasses with ⩾8 wt.% MgO plotted against La/Yb, an indicator of primary melt enrichment or depletion. Error bars are 2σ. Small circles show Iceland (light grey) and Reykjanes Ridge (dark grey) samples with <8 wt.% MgO. The Reykjanes Ridge samples with ⩾8 wt.% MgO are subdivided into those collected at radial distances <620 km (large grey circles) and >620 km (large black circles) from the Iceland plume centre. Iceland melt inclusions are shown in coloured symbols; those with no available La/Yb data are shown to the right of the plot. Kernel density estimates (KDEs) show $\delta^{11}B$ probability distributions for Iceland melt inclusions with MgO⩾8 wt.% (data from Gurenko and Chaussidon, 1997, and this study), glasses from the Reykjanes Ridge, melt inclusions from La Palma and Réunion (Walowski et al., 2019), and melt inclusions from Hawaii (Kobayashi et al., 2004). In the Reykjanes Ridge KDE plot, the black line shows all samples; the red line shows filtered samples collected at radial distance >620 km from the Iceland plume centre (see text for details); the blue line shows samples with radial distance >620 km and MgO⩾8 wt.%, and the dashed orange line shows samples that have B/Pr within the expected MORB range of 0.57 ± 0.09. Shaded grey bar shows the boron isotopic composition of MORB, $\delta^{11}B = -7.1 \pm 0.9$‰, from the compilation of Marschall et al. (2017); the black dashed box shows La/Yb = 1.07 ± 0.89 (2SD) for the same samples. (For interpretation of the references to color in this figure legend, the reader is referred to the web version of this article.)

inclusions (Gurenko and Chaussidon, 1997) within the uncertainty of the measurements. One inclusion from the SW tuff has $\delta^{11}B$ of −10.1‰, similar to the Holuhraun and WVZ inclusions. However, the most probable $\delta^{11}B$ for inclusions from the SW tuff is −5.7‰ (8), indistinguishable from the −6.1‰ of the Reykjanes Ridge glasses within analytical uncertainty.

Our data suggest that Holuhraun and one inclusion from the SW tuff have sampled a common, low-$\delta^{11}B$ mantle component that is characteristic of the Icelandic mantle and distinct from Reykjanes Ridge MORB. There are then two possible explanations for the inclusions from the SW tuff with $\delta^{11}B$ around −5.7‰ and the remaining primitive Holuhraum melt inclusion with $\delta^{11}B$ of −6.4‰. First, these inclusions could have trapped melts that had already assimilated a crustal contaminant with $\delta^{11}B$ higher than −10.6‰. However, the inclusions return OPAM equilibration pressures between 0.58 and 0.40 GPa (~20–14 km, assuming a crustal density of 2860 kg/m^3). This suggests that their host melts had limited opportunity for interaction with altered upper crustal material prior to inclusion trapping. The second, and more likely, explanation is that most of the primitive melt inclusions from the SW tuff, and one inclusion from Holuhraun, have sampled melts of a mantle component with near-identical $\delta^{11}B$ to Reykjanes Ridge MORB.

We modelled the boron contents of the lower- and higher-$\delta^{11}B$ components of the Icelandic mantle using a simple non-modal batch melting model. Relationships between Zr/Y and La/Y suggest that primitve melts from the Askja SW tuff derive from 8–10% partial melting of an approximately 1:1 mixture of melts derived from spinel and garnet peridotites (Fig. S2.16). The average Pr content of primitive inclusions from the SW tuff, 2.3 μg/g, is achieved after 8–10% partial melting of an enriched mantle source containing 0.25 μg/g Pr, similar to primitive mantle (PM) (Pr = 0.27 μg/g; Palme and O'Neill, 2004). The primitive inclusions of the SW tuff have an average B/Pr of 0.30 (range 0.24–0.38), suggesting that the mantle source should contain ~0.083 μg/g B (range 0.066–0.105 μg/g B), similar to DMM. The Zr/Y and La/Y systematics of primitive Holuhraun melt inclusions are best modelled by 10–15% partial melts derived predominantly from spinel-facies mantle (Fig. S2.16). To achieve the average Pr content of primitive Holuhraun melt inclusions (1.5 μg/g) after 15% partial melting, the mantle source should contain ~0.2 μg/g Pr, i.e. intermediate between DMM and PM. The primitive Holuhraun inclusions have an average B/Pr of 0.40 (range 0.38-0.51), suggesting that their mantle source contains ~0.085 μg/g B (range 0.081–0.108 μg/g B). Despite the inherent trade-off between melt fraction and mantle source composition, these simple calculations suggest that the lower- and higher-$\delta^{11}B$ components of the Icelandic mantle have similar B contents around 0.085 μg/g. This suggests that the average Icelandic mantle is slightly enriched in boron compared to average DMM (0.077 ± 0.010 μg/g B; Marschall et al., 2017) and slightly B-depleted compared to Reykjanes Ridge mantle ([B]≈0.10 μg/g), although our estimated ranges for [B] in the Icelandic mantle source overlap both DMM and Reykjanes Ridge mantle. Crucially, these calculations confirm that the incompatible trace element-enriched plume-like component sampled along the northernmost Reykjanes Ridge and by on-land Icelandic basalts shows no enrichment in boron compared to ambient Reykjanes Ridge depleted mantle.

Our new melt inclusion data show a positive correlation between $\delta^{11}B$ and La/Yb, which is often used as a tracer of primary melt enrichment or depletion (Maclennan, 2008) (Fig. 8). This relationship is strengthened if depleted melt inclusions from Miðfell, with low $\delta^{11}B$ and La/Yb<1, are taken into account. We therefore suggest that higher and lower $\delta^{11}B$ signatures in Icelandic primary melts may be associated with incompatible trace element (ITE)-enriched and ITE-depleted mantle components respectively, but both components have similar B contents. They are both intrinsic to the Icelandic mantle source and distinct from ambient depleted Reykjanes Ridge mantle. The presence of an intrinsic depleted Icelandic mantle component distinct from N-MORB is consistent with available trace element and radiogenic isotope data (e.g. Kerr et al., 1995; Fitton et al., 1997; Fitton et al., 2003), while combined Sr-Nd-Pb isotope data suggest the existence of at least four distinct mantle components beneath Iceland that contribute to localised intermediate enriched and depleted components (Thirlwall et al., 2004; Peate et al., 2010). We would expect both depleted and enriched $\delta^{11}B$ signatures to be recorded in early-trapped melt inclusions from individual eruptions, although further measurements of $\delta^{11}B$ in primitive melt inclusions from across Iceland are required to test this hypothesis.

4.5. Recycled boron in the Icelandic mantle source

What is the origin of low $\delta^{11}B$ signatures in primitive Icelandic melt inclusions and the Icelandic mantle source components? Reported $\delta^{11}B$ values for OIB mantle are widely variable, with uncontaminated OIB samples having $\delta^{11}B$ between −12 and −3‰ (Marschall, 2018, and references therein). Ocean island basalts therefore have similar average $\delta^{11}B$ to MORB, but are much more variable, both within and between different locations.

Fig. 8 compares $\delta^{11}B$ in Icelandic melt inclusions with analyses of primitive uncontaminated melt inclusions from La Palma and Réunion (Walowski et al., 2019) and Hawaii (Kobayashi et al., 2004). The modal $\delta^{11}B$ values for the Holuhraun and WVZ melt inclusions, −10.6 and −11.3‰ respectively, are not distinguishable from the La Palma melt inclusions within the uncertainty of *in situ* SIMS measurements. The modal $\delta^{11}B$ for the Hawaii and Réunion melt inclusions are indistinguishable from MORB. The fact that Réunion melt inclusions have $\delta^{11}B$ indistinguishable from MORB led Walowski et al. (2019) to suggest that primitive and depleted upper mantle reservoirs have a common $\delta^{11}B$ signature, and that the low $\delta^{11}B$ values recovered at La Palma and other ocean islands must therefore reflect partial melting of an isotopically distinct mantle component.

Low δ^{11}B values in the La Palma melt inclusions are coupled with radiogenic whole-rock Pb and Os isotopic signatures and low δ^{18}O (Day et al., 2010; Day and Hilton, 2011). These signatures have been interpreted as evidence for recycled oceanic crust and lithosphere in the Canary Islands mantle source, suggesting that the low δ^{11}B could be from a recycled subducted mantle component (Walowski et al., 2019). However, low δ^{11}B is also associated with low B/Zr, indicating that these inclusions are B-depleted relative to melts of typical depleted upper mantle (Walowski et al., 2019).

Simple non-modal batch melting calculations suggest that low B/Pr in North Iceland melt inclusions compared to Reykjanes Ridge or global MORB glasses (Fig. 4f) is consistent with a mantle source with [B] slightly higher than DMM, but slightly lower than Reykjanes Ridge mantle. Importantly, B is not as enriched as trace elements of similar compatibility dring partial melting. This means that neither the isotopically light, incompatible trace element (ITE)-depleted Holuhraun melt inclusions nor the isotopically heavy, ITE-enriched SW tuff melt inclusions can be explained by simple recycling of B-enriched subducted lithologies such as continental sediments or oceanic serpentinites into the mantle, as this would create a source that is both B-enriched and likely isotopically heavy (De Hoog and Savov, 2018).

The best explanation for a B-depleted and isotopically light mantle source component is subducted oceanic lithosphere that has been stripped of its boron through slab dehydration. This is consistent with geochemical and thermodynamic models which predict that subducted oceanic lithosphere will be B-depleted and have δ^{11}B as low as −20 to −40‰, depending on the slab dehydration depth and the thermal profile of the subduction zone (e.g. Peacock and Hervig, 1999; Rosner et al., 2003; Marschall et al., 2007; Konrad-Schmolke and Halama, 2014).

We therefore suggest that the low δ^{11}B sampled by primitive, depleted melt inclusions from Iceland is indictive of dehydrated subducted oceanic lithosphere in an ITE-depleted component intrinsic to the Icelandic mantle (Fig. S2.15). This is consistent with interpretations of major, trace and lithophile isotope systematics in Icelandic basalts, which have likewise inferred the presence of at least 5% recycled material in the Icelandic mantle (e.g. Chauvel and Hémond, 2000; Stracke et al., 2003; Thirlwall et al., 2004; Kokfelt et al., 2006; Bindeman et al., 2008; Shorttle et al., 2014), and that ancient depleted oceanic lithospheric mantle is a plausible source for the intrinsic depleted Iceland component (e.g. Skovgaard et al., 2001, Fitton et al., 2003, and references therein). Melt inclusions sampling this depleted component show no B enrichment compared to Reykjanes Ridge basalts. This suggests that the recycled lithospheric component is likely boron-poor, and hence recycled boron is difficult to detect other than by its low boron isotopic signature. The enriched mantle component sampled by ITE-enriched melt inclusions is also likely to contain dehydrated lithosphere. However, the recycled lithospheric component in the enriched mantle source likely contains almost no boron, meaning that melt boron content is diluted by the recycled component rather than enriched. The boron isotopic signatures of melts from the enriched component are therefore dominated by ambient depleted upper mantle and hence very similar to Rekjanes Ridge basalts and global MORB.

5. MODIFICATION OF MELT δ^{11}B THROUGH ASSIMILATION OF ALTERED CRUST

The North Iceland melt inclusions have major and trace element contents that are broadly consistent with a dominant fractional crystallization control (Hartley and Thordarson, 2013). However, some melt inclusions with <8 wt.% MgO have higher δ^{11}B than Reykjanes Ridge MORB, while others are isotopically ligher than primitive North Iceland melt inclusions (Fig. 8; Fig. S9). Given that a small number of North Iceland melt inclusions show signatures of minor B addition independent of Pr (Fig. 4) that are inconsistent with simple fractional crystallization, we explore whether the North Iceland melt inclusions could have assimilated a high-[B] component with heterogeneous δ^{11}B.

The well-defined correlation between δ^{18}O and indices of melt evolution in our North Iceland samples (Fig. 6b, Fig. S2.10) is not consistent with high-temperature fractional crystallization, since this process is not expected to fractionate oxygen isotopes (e.g. Bindeman et al., 2008). The major and trace element systematics of the North Iceland melt inclusions are not consistent with mixing between basaltic melt and low-δ^{18}O rhyolitic or andesitic magmas. Instead, the low δ^{18}O signatures are best explained through bulk assimilation of altered basaltic hyaloclastite in the upper crust and/or mixing with low-δ^{18}O basaltic melts stored in upper crustal reservoirs (Hartley et al., 2013). Low δ^{18}O in olivine and plagioclase crystals from large-volume Holocene lavas in Iceland's Eastern Volcanic Zone have likewise been interpreted as resulting from bulk digestion of low-δ^{18}O basaltic hyaloclastite, whereby the hyaloclastite inherits its oxygen isotopic signature through interaction with low-δ^{18}O glacial meltwaters (Bindeman et al., 2006; Bindeman et al., 2008). Given that melt inclusion δ^{18}O signatures require assimilation of an altered crustal component, we examine whether variable δ^{11}B in the North Iceland melt inclusions can also be generated through crustal assimilation.

Published measurements of δ^{11}B in Icelandic upper crustal materials are restricted to a single drill core RN-17 from the Reykjanes Peninsula (Raffone et al., 2010). Basalts sampled between 0 and 3000 m in this core have high whole-rock B contents of 3.3–12.4 μg/g and heterogeneous δ^{11}B between −18.3 and −4.4‰, and there is no correlation between [B] and δ^{11}B, nor between composition and depth (Raffone et al., 2008; Raffone et al., 2010) (Fig. 7). Boron in the RN-17 samples is primarily concentrated in hydrothermal minerals including epidote (0.3–9.0 μg/g) and amphibole (0.1–2.3 μg/g); however, the abundance of hydrothermal minerals is too low to explain the elevated bulk B contents. Brounce et al. (2012) proposed that the

Table 1
Mixing model endmembers and reference values.

Endmember	B, μg/g	δ^{11}B, ‰	W/R[a]	Reference
N-MORB	0.5	−7.1		Marschall et al. (2017)
Holuhraun primitive melt inclusions	0.42	−10.6		
SW tuff primitive melt inclusions	0.57	−5.7		
Mean seawater-altered oceanic crust	5.2	3.4		Smith et al. (1995)
Reykjanes RN-17 drill core, 400 m	6.06	−6.4		Raffone et al. (2010)
Reykjanes RN-17 drill core, 650 m	11.38	−4.4		Raffone et al. (2010)
Reykjanes RN-17 rill core, 750 m	5.51	−7.7		Raffone et al. (2010)
Model hyaloclastite[b] Hy-1	1.3	14.4	1.5[c]	
Model hyaloclastite[b] Hy-2	2.9	−25.0	10[d]	
Model hyaloclastite[b] Hy-3	3.6	3.1	1.85[e]	
Model hyaloclastite[b] Hy-4	3.8	−12.7	4[c]	
Mean Iceland geothermal fluid	2.8	−3.7		Aggarwal et al. (2000)
Krafla geothermal fluid 1	1.45	−6.5		Aggarwal et al. (2000)
Krafla geothermal fluid 2	5.71	−6.7		Aggarwal et al. (2000)

[a] Water/rock ratio.
[b] Calculated using adsorption coefficient $K_d = 2.6$ and isotopic fractionation factor $\alpha = 0.975$ (Palmer et al., 1987).
[c] Fluid composition is mean Icelandic geothermal fluid, an average of three active high-temperature geothermal sites sampled over the course of 8 years.
[d] Fluid composition is Krafla geothermal fluid 1.
[e] Fluid composition is Krafla geothermal fluid 2.

additional boron is concentrated on altered surfaces within porous altered basalt.

We have modelled the generation of B-rich altered basaltic hyaloclastites in the upper crust following the two-stage process described by Brounce et al. (2012). First, B-depleted meteoric fluids circulating through high-temperature geothermal systems in the upper crust scavenge B from the basalts they flow through. Meteoric and glacial waters across Iceland typically contain <0.3 μg/g B and have high δ^{11}B up to +17‰. In contrast, high-temperature geothermal waters contain up to 5 μg/g B and have δ^{11}B down to −6.7‰ (Aggarwal et al., 2000) (Table 1, Fig. S2.14), suggesting that boron scavenging during high-temperature fluid-rock interaction is associated with isotopic fractionation of several permil. Second, the fluids cool to temperatures <200 °C at which point scavenged B adsorbs onto clay mineral surfaces in palagonitized basaltic hyaloclastite, predominantly smectite and illite, driving the bulk rock towards high [B]. Boron isotopes are further fractionated during adsorption, since ^{10}B is adsorbed preferentially to ^{11} B in clay minerals (Palmer et al., 1987). The boron content and δ^{11}B of the resultant altered basaltic hyaloclastite is controlled by four factors: the composition of the circulating hydrothermal fluid; the adsorption coefficient; the isotopic fractionation factor; and the water–rock ratio. Following Brounce et al. (2012), we assume that the boron adsorption coefficient $K_d = 2.6$ and fractionation factor $\alpha = 0.975$ for marine clays at 25°C and pH = 7.8 (Palmer et al., 1987) are appropriate for boron adsorption onto the smectite-dominated clay mineral assemblages present in palagonitized basaltic hyaloclastite. The isotopic ratio of the altered hyaloclastite is then calculated as a function of water/rock ratio W/R (Spivack and Edmond, 1987):

$$\delta^{11}B_R = \alpha(\delta^{11}B_W + 10^3)\exp\left[\frac{K_d(1-\alpha)}{W/R}\right] - 10^3 \quad (2)$$

where the subscript R refers to the rock, and the subscript W refers to the hydrothermal fluid. Similarly, the boron concentration in the altered hyaloclastite is calculated as follows:

$$[B]_R = [B]_W \cdot K_d \cdot \exp\left(\frac{-K_d}{W/R}\right) \quad (3)$$

Table 1 shows a selection of potential compositions of altered basaltic hyaloclastites, including model hyaloclastite compositions calculated using different fluid compositions and water–rock ratios. Water-rock ratios >4 are required to generate materials with high [B] and low δ^{11}B, similar to altered basalts in the RN-17 core (Raffone et al., 2008). Water–rock ratios <3 generate materials with lower [B] and higher δ^{11}B than typical MORB (Fig. S2.14).

We have used a range of possible natural and modelled crustal endmember compositions to calculate parabolic mixing curves to model the likely effects of crustal assimilation on [B], δ^{11}B and δ^{18}O on North Iceland melts (Fig. 9). The primitive melt endmembers in our mixing models are the compositions of primitive melt inclusions from Holuhraun and the Askja SW tuff, with δ^{11}B of −10.6‰ and −5.7‰ respectively (Fig. 8). The oxygen isotopic ratio of altered basaltic hyaloclastite is difficult to constrain and likely to be heterogeneous in the upper crust. Hyaloclastites from the KG-4 Krafla drill hole have δ^{18}O between −10.3 and −3.4‰ (Hattori and Muehlenbachs, 1982), while rhyolitic tephra and leucocratic xenoliths from the Askja 1875 eruption have δ^{18}O between −7.50 and +1.65‰ (Macdonald et al., 1987). For simplicity, the mixing curves in Fig. 9b assume δ^{18}O of −4‰ for all crustal endmembers.

Our bulk mixing models suggest that [B], δ^{11}B and δ^{18}O in melt inclusions and glasses from North Iceland can be derived by assimilation of up to ~20% altered crustal material, with most melt inclusion compositions requiring <10% assimilation (Fig. 9). The choice of primitive melt

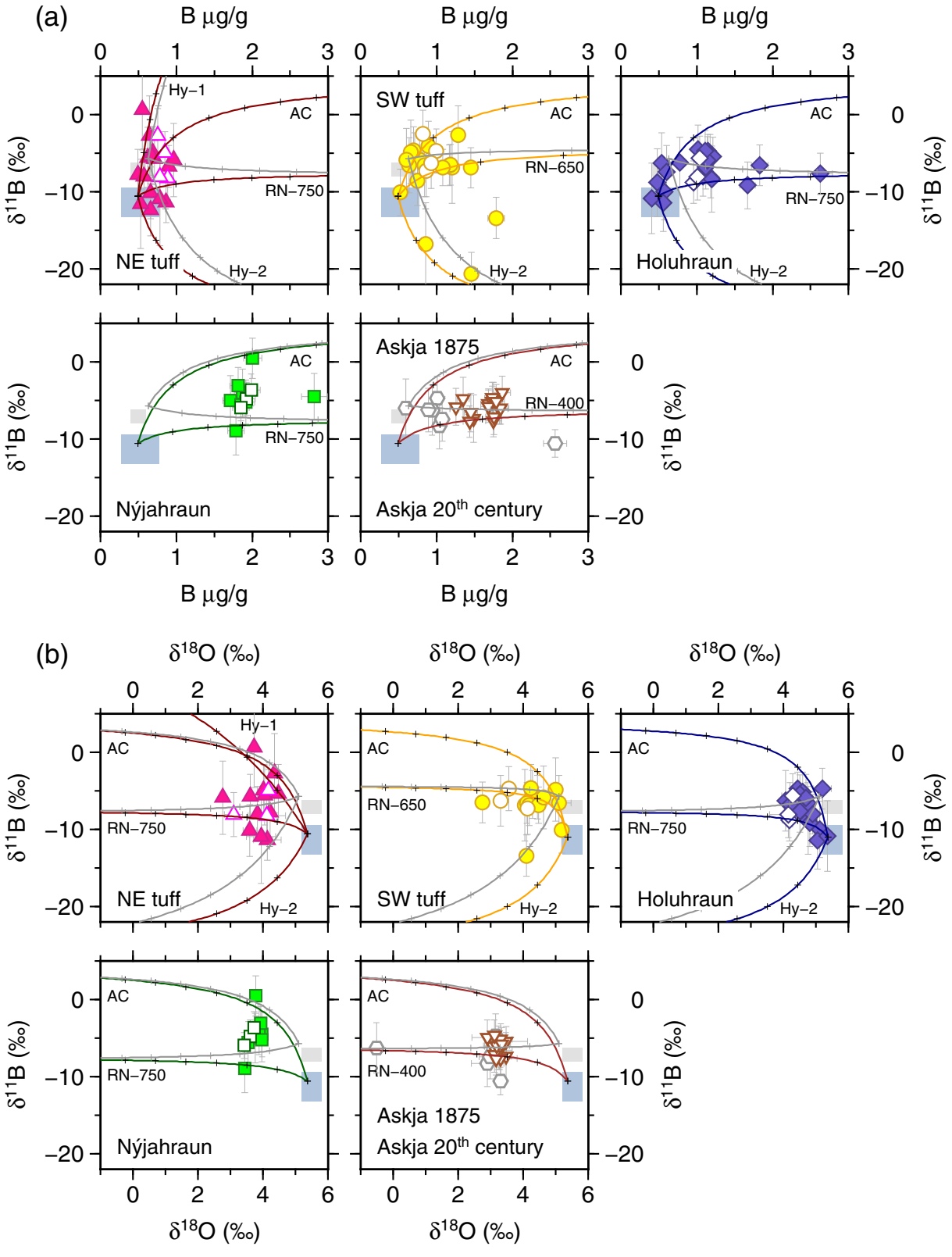
(a)
B µg/g
δ11B (‰)
Hy–1
AC
RN–750
NE tuff
Hy–2
SW tuff
RN–650
Holuhraun
Askja 1875
RN–400
Nýjahraun
Askja 20th century
(b)
δ18O (‰)

endmember composition makes little difference to the degree of assimilation required to explain the observed boron and oxygen isotopic variations. Compositions similar to the primitive SW tuff melt inclusions can be generated by <5% contamination of the recycled endmember, which could support an argument that their $\delta^{11}B$ of −5.7‰ does not represent a primary mantle component, but is instead generated through very small degrees of crustal assimilation. However, melt inclusions from the SW tuff are trapped at pressures >0.4 GPa in the mid- to lower crust (Fig. 7), and are therefore unlikely to have interacted with high-[B] altered crustal material. The boron isotopic compositions of primitive North Iceland melt inclusions are therefore best explained by differential sampling of a heterogeneous mantle containing a Reykjanes Ridge-like mantle component with $\delta^{11}B$ around −6‰ and a recycled component with $\delta^{11}B$ around −11‰.

Mixing curves calculated between the recycled mantle endmember and plausible crustal endmembers can account for the full variety of melt inclusion and glass compositions (Fig. 9). In contrast, mixing curves calculated using a Reykjanes Ridge-like primary melt endmember do not satisfactorily reproduce [B], $\delta^{11}B$ and $\delta^{18}O$ for the most primitive Holuhraun melt inclusions, nor a subset of low-$\delta^{11}B$ inclusions from Askja NE and SW tuff sequences. Our data therefore strongly support the presence of a recycled component in the Icelandic mantle source with $\delta^{11}B$ around −11‰. Evolved melt inclusions with $\delta^{11}B$ values higher than typical Reykjanes Ridge MORB or lower than the primitive Holuhraun inclusions are generated through minor assimilation of heterogeneous altered material distributed through the upper crust.

6. CONCLUSIONS

We have reported new measurements of volatiles, light elements and boron isotopes in a suite of melt inclusions from North Iceland, and in submarine glasses from the Reykjanes Ridge. Reykjanes Ridge glasses sampled at radial distances >620 km from the Iceland plume show no evidence of enrichment from a plume-derived mantle component, and from these samples we derive a new estimate for the $\delta^{11}B$ signature of Reykjanes Ridge mantle, of −6.1‰ (2SD = 1.5‰, 2SE = 0.3‰, $n = 21$). We find only a very weak indication of along-ridge enrichment in [B] approaching Iceland, and no systematic variation in $\delta^{11}B$ along the entire ridge segment. This suggests that the enriched mantle component sampled by the northern ridge segment close to Iceland is not contributing substantially to the boron budget of these melts.

Olivine- and plagioclase-hosted melt inclusions from North Iceland have major element compositions that are broadly consistent with fractional crystallization. Ratios of volatiles and light elements to similarly incompatible trace elements indicate that melt inclusion volatile contents are broadly consistent with canonical mantle reservoirs and, with the exception of CO_2, have experienced minimal pre-, syn- and/or post-entrapment modification. A small number of melt inclusions have higher [B] than is consistent with simple fractional crystallization trends, indicating assimilation of a B-rich component prior to melt inclusion trapping.

The North Iceland melt inclusions are characterized by widely variable $\delta^{11}B$ values between −20.7 and +0.6‰. The coupled [B], $\delta^{11}B$ and $\delta^{18}O$ signatures of more evolved melt inclusions are consistent with progressive assimilation of hydrothermally altered basaltic hyaloclastite as they ascend through the upper crust. Altered basaltic hyaloclastites in the Icelandic upper crust have high [B] and highly heterogeneous $\delta^{11}B$ in comparison to pristine Icelandic basalts. Even small degrees of crustal assimilation could thus exert a strong control on the bulk $\delta^{11}B$ of ascending magmas, generating wide $\delta^{11}B$ variability within a single sample set. To access mantle-derived $\delta^{11}B$ signatures, we identify and exclude any melt inclusions that may have been modified by crustal processing. Our observations suggest that only the most primitive melt inclusions reliably record truly primitive $\delta^{11}B$ signatures. Our unfiltered North Iceland melt inclusion dataset records the same large range in $\delta^{11}B$ as other oceanic islands such as Hawaii (Kobayashi et al., 2004), which highlights the importance of very careful screening of melt inclusion compositions in order to study global crustal recycling in ocean island basalts.

Simple non-modal batch melting calculations suggest that the Icelandic mantle contains ~0.085 μg/g B, slightly lower than the 0.10–0.11 μg/g calculated for depleted Reykjanes Ridge mantle. The lowest $\delta^{11}B$ signatures in Icelandic melt inclusions are typically associated with more primitive (MgO ⩾ 8 wt.%) and ITE-depleted melt compositions. Primitive melt inclusions from Holuhraun record a primary melt $\delta^{11}B$ of −10.6‰, consistent with melting of a depleted

Fig. 9. (a) Boron concentrations and isotopic compositions of melt inclusions and glasses from North Iceland. (b) Boron and oxygen isotopic compositions of melt inclusions and glasses from North Iceland. Error bars are 2σ. The shaded boxes show the expected compositions of unmodified primary melts from MORB (grey, Marschall et al. (2017)) and Iceland (this study, light blue) mantle sources. Parabolic mixing curves are calculated between a primitive endmember and a range of potential crustal assimilants (Table 1). The primitive endmembers are taken to be the mean composition of primitive Holuhraun melt inclusions (coloured curves) or the mean composition of primitive inclusions from the SW tuff (grey curves). The mixing curves in (b) assume that the crustal assimilants have $\delta^{18}O$ of −4‰, consistent with basaltic hyaloclastites obtained from the Krafla KG-4 drill hole (Hattori and Muehlenbachs, 1982). Crosses show 5% increments of assimilation. Most melt inclusion and glass compositions can be modelled by up to 15% assimilation of likely crustal components. (For interpretation of the references to color in this figure legend, the reader is referred to the web version of this article.)

mantle component containing dehydrated recycled oceanic lithosphere. This low-δ^{11}B depleted mantle component is also recorded in melt inclusions from the WVZ and Reykjanes Peninsula. The δ^{11}B of −5.7‰ recorded in primitive, ITE-enriched melt inclusions is consistent with an enriched mantle lithology that has similar boron isotopic composition to Reykjanes Ridge mantle. Our data therefore confirm the presence of boron isotopic heterogeneity in the Icelandic mantle source. We have not recovered boron isotopic heterogeneity on the lengthscale of melt supply to a single eruption, but our data do not exclude this possibility and this question may be revisited as more measurements of primitive melt inclusions become available and as *in situ* analytical techniques are improved. Our verification of a low-δ^{11}B recycled component in the Icelandic mantle provides further support for the role of recycled subducted oceanic lithosphere in melt generation at ocean islands.

Declaration of Competing Interest

The authors declare that they have no known competing financial interests or personal relationships that could have appeared to influence the work reported in this paper.

ACKNOWLEDGEMENTS

Access to the Edinburgh Ion Microprobe Facility was supported by the Natural Environment Research Council under proposals [IMF504/1013] and [IMF515/0514]. MEH acknowledges support from a Junior Research Fellowship at Murray Edwards College, Cambridge, the Royal Society [130438], and NERC [NE/P002331/1]. OS acknowledges support from a Junior Research Fellowship at Trinity College, Cambridge. We acknowledge the National Oceanographic Centre, the PETROS project, and Bramley Murton for providing the Reykjanes Ridge samples. We thank Marc Chaussidon, Horst Marschall, Andrey Gurenko and the Associate Editor for their detailed reviews and helpful suggestions.

APPENDIX A. SUPPLEMENTARY MATERIAL

Supplementary data associated with this article can be found, in the online version, at https://doi.org/10.1016/j.gca.2020.11.013.

REFERENCES

Aggarwal J. K., Palmer M. R., Bullen T. D., Arnórsson S. and Ragnarsdóttir K. V. (2000) The boron isotope systematics of Icelandic geothermal waters: 1. Meteoric water charged systems. *Geochim. Cosmochim. Acta* **64**, 579–585.

Allègre C. J. and Turcotte D. L. (1986) Implications of a two-component marble-cake mantle. *Nature* **323**, 123–127.

Bali E., Hartley M. E., Halldórsson S. A., Gudfinnsson G. H. and Jakobsson S. (2018) Melt inclusion constraints on volatile systematics and degassing history of the 2014–2015 Holuhraun eruption, Iceland. *Contrib. Mineral. Petrol.* **173**, 9.

Bindeman I., Gurenko A., Sigmarsson O. and Chaussidon M. (2008) Oxygen isotope heterogeneity and disequilibria of olivine crystals in large volume Holocene basalts from Iceland: evidence for magmatic digestion and erosion of Pleistocene hyaloclastites. *Geochim. Cosmochim. Acta* **72**, 4397–4420.

Bindeman I. N., Sigmarsson O. and Eiler J. M. (2006) Time constraints on the origin of large volume basalts derived from O-isotope and trace element mineral zoning and U-series disequilibria in the Laki and Grímsvötn volcanic system. *Earth Planet. Sci. Lett.* **245**, 245–259.

Brenan J. M., Neroda E., Lundstrom C. C., Shaw H. F., Ryerson F. J. and Phinney D. L. (1998) Behaviour of boron, beryllium, and lithium during melting and crystallization: constraints from mineral-melt partitioning experiments. *Geochim. Cosmochim. Acta* **62**, 2129–2141.

Brounce M., Feineman M., LaFemina P. and Gurenko A. (2012) Insights into crustal assimilation by Icelandic basalts from boron isotopes in melt inclusions from the 1783–1784 Lakagígar eruption. *Geochim. Cosmochim. Acta* **94**, 164–180.

Chaussidon M. and Jambon A. (1994) Boron content and isotopic composition of oceanic basalts: geochemical and cosmochemical implications. *Earth Planet. Sci. Lett.* **121**, 277–291.

Chaussidon M. and Marty B. (1995) Primitive boron isotope composition of the mantle. *Science* **269**, 383–386.

Chauvel C. and Hémond C. (2000) Melting of a complete section of recycled oceanic crust: trace element and Pb isotopic evidence from Iceland. *Geochem. Geophys. Geosyst.* **1**, 1001. https://doi.org/10.1029/1999GC000002.

Darbyshire F. A., Priestley K. F., White R. S., Stefansson R., Gudmundsson G. B. and Jakobsdottir S. S. (2000) Crustal structure of central and northern Iceland from analysis of teleseismic receiver functions. *Geophys. J. Int.* **143**, 163–184.

Day J. M. D. and Hilton D. R. (2011) Origin of ^{3}He/^{4}He ratios in HIMU-type basalts constrained from Canary Island lavas. *Earth Planet. Sci. Lett.* **305**, 226–234.

Day J. M. D., Pearson D. G., Macpherson C. G., Lowry D. and Carracedo J.-C. (2010) Evidence for distinct proportions of subducted oceanic crust and lithosphere in HIMU-type mantle beneath El Hierro and La Palma, Canary Islands. *Geochim. Cosmochim. Acta* **74**, 6565–6589.

De Hoog J. C. M. and Savov I. P. (2018) Subduction zones, dehydration, metasomatism, mud and serpentinite volcanoes, and arc magmatism. *Adv. Geochem.*, 217–247.

Dixon J. E. and Clague D. A. (2001) Volatiles in basaltic glasses from Loihi Seamount, Hawaii: Evidence for a relatively dry plume component. *J. Petrol.* **42**, 627–654.

Edmonds M. (2015) Partitioning of light lithophile elements during basalt eruptions on Earth and application to Martian shergottites. *Earth Planet. Sci. Lett.* **411**, 142–150.

Eiler J. M. (2001) Oxygen isotope variations of basaltic lavas and upper mantle rocks. *Rev. Mineral. Geochem.* **43**, 319–364.

Fitton J. G., Saunders A. D., Kempton P. D. and Hardarson B. S. (2003) Does depleted mantle form an intrinsic part of the Iceland plume? *Geochem. Geophys. Geosyst.* **4**, 1032. https://doi.org/10.1029/2002GC000424.

Fitton J. G., Saunders A. D., Norry M. J., Hardarson B. S. and Taylor R. N. (1997) Thermal and chemical structure of the Iceland plume. *Earth Planet. Sci. Lett.* **153**, 197–208.

Greenfield T. and White R. S. (2015) Building Icelandic igneous crust by repeated melt injections. *J. Geophys. Res. Solid Earth* **120**, 7771–7788. https://doi.org/10.1002/2015JB012009.

Gurenko A. A. and Chaussidon M. (1995) Enriched and depleted primitive melts included in olivine from Icelandic tholeiites: origin by continuous melting of a single mantle column. *Geochim. Cosmochim. Acta* **59**, 2905–2917.

Gurenko A. A. and Chaussidon M. (1997) Boron concentrations and isotopic composition of the Icelandic mantle: evidence from glass inclusions in olivine. *Chem. Geol.* **135**, 21–34.

Halldorsson S. A., Óskarsson N., Grönvold K., Sigurdsson G., Sverrisdóttir G. and Steinthórsson S. (2008) Isotopic-heterogeneity of the Thjorsa lava: Implications for mantle sources and

crustal processes within the Eastern Rift Zone, Iceland. *Chem. Geol.* **255**, 305–316.

Hanan B. B. and Schilling J.-G. (1997) The dynamic evolution of the Iceland mantle plume: the lead isotope perspective. *Earth Planet. Sci. Lett.* **151**, 43–60.

Hart R., Dymond J., Hogan L. and Schilling J.-G. (1983) Mantle plume noble gas component in glassy basalts from Reykjanes Ridge. *Nature* **305**, 403–407.

Hartley M. E., Bali E., Maclennan J., Neave D. A. and Halldórsson S. A. (2018) Melt inclusion constraints on petrogenesis of the 2014–2015 Holuhraun eruption, Iceland. *Contrib. Miner. Petrol.* **173**, 10.

Hartley M. E., Maclennan J., Edmonds M. and Thordarson T. (2014) Reconstructing the deep CO_2 degassing behaviour of large basaltic fissure eruptions. *Earth Planet. Sci. Lett.* **393**, 120–131.

Hartley M. E., Neave D. A., Maclennan J., Edmonds M. and Thordarson T. (2015) Diffusive over-hydration of olivine-hosted melt inclusions. *Earth Planet. Sci. Lett.* **425**, 168–178.

Hartley M. E. and Thordarson T. (2013) The 1874–76 volcano-tectonic episode at Askja, North Iceland: Lateral flow revisited. *Geochem. Geophys. Geosyst.* **14**, 2286–2309. https://doi.org/10.1002/ggge.20151.

Hartley M. E., Thordarson T., Fitton J. G. and EIMF (2013) Oxygen isotopes in melt inclusions and glasses from the Askja volcanic system, North Iceland. *Geochim. Cosmochim. Acta* **123**, 55–73.

Hartley M. E., Thordarson T., Taylor C., Fitton J. G. and EIMF (2012) Evaluation of the effects of composition on instrumental mass fractionation during SIMS oxygen isotope analyses of glasses. *Chem. Geol.* **334**, 312–323.

Hattori K. and Muehlenbachs K. (1982) Oxygen isotope ratios of the Icelandic crust. *J. Geophys. Res.* **87**, 6559–6565.

Hauri E. H., Maclennan J., McKenzie D., Gronvold K., Oskarsson N. and Shimizu N. (2018) CO_2 content beneath northern Iceland and the variability of mantle carbon. *Geology* **46**, 55–58.

Hirschmann M. M. and Stolper E. M. (1996) A possible role for garnet pyroxenite in the origin of the "garnet signature" in MORB. *Contrib. Miner. Petrol.* **124**, 185–208.

Jackson M. G., Weis D. and Huang S. (2012) Major element variations in Hawaiian shield lavas: Source features and perspectives from global ocean island basalt (OIB) systematics. *Geochemis. Geophys. Geosyst.* **13**, Q09009. https://doi.org/10.1029/2012GC004268.

Kawakami Y., Yamamoto J. and Kagi H. (2003) Micro-Raman densimeter for CO_2 inclusions in mantle-derived minerals. *Appl. Spectrosc.* **57**, 1333–1339.

Kellogg L. H. and Turcotte D. L. (1987) Homogenization of the mantle by convective mixing and diffusion. *Earth Planet. Sci. Lett.* **81**, 371–378.

Kendrick M. A., Jackson M. G., Kent A. J. R., Hauri E. H., Wallace P. J. and Woodhead J. (2015) Contrasting behaviours of CO_2, S, H_2O and halogens (F, Cl, Br, and I) in enriched-mantle melts from Pitcairn and Society seamounts. *Chem. Geol.* **370**, 69–81.

Kerr A. C., Saunders A. D., Tarney J., Berry V. L. and Hards N. H. (1995) Depleted mantle-plume geochemical signatures: No paradox for plume theories. *Geology* **23**, 843–846.

Kobayashi K., Tanaka R., Moriguti T., Shimizu K. and Nakamura E. (2004) Lithium, boron, and lead isotope systematics of glass inclusions in olivines from Hawaiian lavas: evidence for recycled components in the Hawaiian plume. *Chem. Geol.* **212**, 143–161.

Kokfelt T. F., Hoernle K., Hauff F., Fiebig J., Werner R. and Garbe-Scönberg D. (2006) Combined trace element and Pb-Nd-Sr-O isotope evidence for recycled oceanic crust (upper and lower) in the Iceland mantle plume. *J. Petrol.* **47**, 1705–1749.

Konrad-Schmolke M. and Halama R. (2014) Combined thermodynamic-geochemical modeling in metamorphic geology: boron as tracer of fluid–rock interaction. *Lithos* **208**, 393–414.

Koornneef J. M., Stracke A., Bourdon B. and Grönvold K. (2012) The influence of source heterogeneity on the U-Th-Pa-Ra disequilibria in post-glacial tholeiites from Iceland. *Geochim. Cosmochim. Acta* **87**, 243–266.

Koornneef J. M., Stracke A., Bourdon B., Meier M. A., Jochum K. P., Stoll B. and Grönvold K. (2012) Melting of a two-component source beneath Iceland. *J. Petrol.* **53**, 127–157.

Langmuir C. H. and Hanson G. N. (1980) An evaluation of major element heterogeneity in the mantle sources of basalts. *Philos. Trans. R. Soc. Lond. Ser. A* **297**, 383–407.

Macdonald R., Sparks R. S. J., Sigurdsson H., Mattey D. P., McGarvie D. W. and Smith R. L. (1987) The 1875 eruption of Askja volcano, Iceland: combined fractional crystallisation and selective contamination in the generation of rhyolitic magma. *Mineral. Mag.* **51**, 183–202.

Maclennan J. (2008) Concurrent mixing and cooling of melts under Iceland. *J. Petrol.* **49**, 1931–1953.

Maclennan J. (2008) Lead isotope variability in olivine-hosted melt inclusions from Iceland. *Geochim. Cosmochim. Acta* **72**, 4159–4176.

Maclennan J. (2017) Bubble formation and decrepitation control the CO_2 content of olivine-hosted melt inclusions. *Geochem. Geophys. Geosyst.* **18**, 597–616.

Maclennan J., McKenzie D., Hilton F., Grönvold K. and Shimizu N. (2007) 2003: Geochemical variability in a single flow from northern Iceland. *J. Geophys. Res.* **108**. https://doi.org/10.1029/2000JB000142.

Marschall H. R. (2018) Boron isotopes in the ocean floor realm and the mantle. In Boron Isotopes: The Fifth Element (eds. M.H.R. and F.G.L.). Springer. pp. 189–215.

Marschall H. R., Altherr R. and Rüpke L. (2007) Squeezing out the slab–modelling the release of Li, Be and B during progressive high-pressure metamorphism. *Chem. Geol.* **239**, 323–335.

Marschall H. R., Wanless V. D., Shimizu N., Pogge von Strandmann P. A. E., Elliott T. and Monteleone B. D. (2017) The boron and lithium isotopic composition of mid-ocean ridge basalts and the mantle. *Geochim. Cosmochim. Acta* **207**, 102–138.

Matthews S., Shorttle O., Rudge J. F. and Maclennan J. (2017) Constraining mantle carbon: CO_2-trace element systematics in basalts and the roles of magma mixing and degassing. *Earth Planet. Sci. Lett.* **480**, 1–14.

Michael P. J. (1995) Regionally distinctive sources of depleted MORB: Evidence from trace elements and H_2O. *Earth Planet. Sci. Lett.* **131**, 301–320.

Michael P. J. and Cornell W. C. (1998) Influence of spreading rate and magma supply on crystallization and assimilation beneath mid-ocean ridges: Evidence from chlorine and major element chemistry of mid-ocean ridge basalts. *J. Geophys. Res. Solid Earth* **103**, 18325–18356.

Michael P. J. and Graham, D. W. (2013) Concentration and behavior of CO_2 in MORB and OIB: a reevaluation. Goldschmidt 2013 Conference Abstracts, 1752, doi:10.1180/minmag.2013.077.5.13.

Michael P. J., Graham D. W., Michael P. J. and Graham D. W. (2015) The behavior and concentration of CO_2 in the suboceanic mantle: Inferences from undegassed ocean ridge and ocean island basalts. *Lithos* **236**, 338–351.

Miller W. G. R., Maclennan J., Shorttle O., Gaetani G. A., Le Roux V. and Klein F. (2019) Estimating the carbon content of the deep mantle with Icelandic melt inclusions. *Earth Planet. Sci. Lett.* **523**, 115699.

Murton B. J. (1995) RRS Charles Darwin Cruise CD80, 01 Sep-01 Oct 1993. The PETROS Programme (PETRogenesis of Oblique Spreading). Institute of Oceanographic Sciences, Deacon Laboratory, 241, 77 pp.

Murton B. J., Taylor R. N. and Thirlwall M. F. (2002) Plume-ridge interaction: a geochemical perspective from the Reykjanes Ridge. *J. Petrol.* **43**, 1987–2012.

Neave D. A., Hartley M. E., Maclennan J., Edmonds M. and Thordarson T. (2017) Volatile and light lithophile elements in high-anorthite plagioclase-hosted melt inclusions from Iceland. *Geochim. Cosmochim. Acta* **205**, 100–118.

Neave D. A., Maclennan J., Edmonds M. and Thordarson T. (2014) Melt mixing causes negative correlation of trace element enrichment and CO_2 content prior to an Icelandic eruption. *Earth Planet. Sci. Lett.* **400**, 272–283.

Neave D. A., Passmore E., Maclennan J., Fitton G. and Thordarson T. (2013) Crystal-melt relationships and the record of deep mixing and crystallization in the AD 1783 Laki eruption, Iceland. *J. Petrol.* **54**, 1661–1690.

Nichols A. R. L., Carroll M. R. and Hóskuldsson A. (2002) Is the Iceland hot spot also wet? Evidence from the water contents of undegassed submarine and subglacial pillow basalts. *Earth Planet. Sci. Lett.* **202**, 77–87.

Novella D., Maclennan J., Shorttle O., Prytulak J. and Murton B. J. (2020) A multi-proxy investigation of mantle oxygen fugacity along the Reykjanes Ridge. *Earth Planet. Sci. Lett.* **531**, 115973.

O'Neill H. S. C. and Jenner F. E. (2012) The global pattern of trace-element distributions in ocean floor basalts. *Nature* **491**, 698–704.

Palme H. and O'Neill H. S. C. (2004) Cosmochemical estimates of mantle composition. In *Treatise on Geochemistry*, vol. 2 (eds. H. D. Holland and K. K. Turrekian). Elsevier, pp. 1–38.

Palmer M. R., Spivack A. J. and Edmond J. M. (1987) Temperature and pH controls over isotopic fractionation during adsorption of boron on marine clay. *Geochim. Cosmochim. Acta* **51**, 2319–2323.

Peacock S. M. and Hervig R. L. (1999) Boron isotopic composition of subduction-zone metamorphic rocks. *Chem. Geol.* **160**, 281–290.

Peate D. W., Breddam K., Baker J. A., Kurz M. D., Barker A. K., Prestvik T., Grassineau N. and Skovgaard A. C. (2010) Compositional characteristics and spatial distribution of enriched Icelandic mantle components. *J. Petrol.* **51**, 1447–1475.

Pedersen G. B. M., Höskuldsson A., Dürig T., Thordarson T., Jónsdóttir I., Riishuus M. S., Óskarsson B. V., Dumont S., Magnússon E., Gudmundsson M. T., Sigmundsson F., Drouin V. J. P. B., Gallagher C., Askew R., Gudnason J., Moreland W. M., Nikkola P., Reynolds H. I., Schmith J. and IES eruption team (2017) Lava field evolution and emplacement dynamics of the 2014–2015 basaltic fissure eruption at Holuhraun, Iceland. *J. Volcanol. Geoth. Res.* **340**, 155–169.

Prytulak J. and Elliott T. (2007) TiO_2 enrichment in ocean island basalts. *Earth Planet. Sci. Lett.* **263**, 388–403.

Putirka K. D. (2008) Thermometers and barometers for volcanic systems. *Rev. Mineral. Geochem.* **69**, 61–120.

Raffone N., Ottolini L., Tonarini S., Gianelli G. and Fridleifsson G. Ó. (2008) A SIMS study of lithium, boron and chlorine in basalts from Reykjanes (southwestern Iceland). *Microchim. Acta* **161**, 307–312.

Raffone N., Ottolini L. P., Tonarini S., Gianelli G., D'Orazio M. and Fridleifsson G. Ó. (2010) An investigation of trace and isotope light elements in mineral phases from well RN-17 (Reykjanes Peninsula, SW Iceland). *IOP Conf. Ser. Mater. Sci. Eng.* **7**, 012026.

Roeder P. L. and Emslie R. F. (1970) Olivine-liquid equilibrium. *Contrib. Miner. Petrol.* **29**, 275–289.

Rose-Koga E. F. and Sigmarsson O. (2008) B-O-Th isotope systematics in Icelandic tephra. *Chem. Geol.* **255**, 454–462.

Rosenthal A., Hauri E. H. and Hirschmann M. M. (2015) Experimental determination of C, F, and H partitioning between mantle minerals and carbonated basalt, CO_2/Ba and CO_2/Nb systematics of partial melting, and the CO_2 contents of basaltic source regions. *Earth Planet. Sci. Lett.* **412**, 77–87.

Rosner M., Erzinger J., Franz G. and Trumbull R. B. (2003) Slab-derived boron isotope signatures in arc volcanic rocks from the Central Andes and evidence for boron isotope fractionation during progressive slab dehydration. *Geochem. Geophys. Geosyst.* **4**. https://doi.org/10.1029/2002GC000438.

Ryan J. G. and Langmuir C. H. (1987) The systematics of lithium abundances in young volcanic rocks. *Geochim. Cosmochim. Acta* **51**, 1727–1741.

Ryan J. G., Leeman W. P., Morris J. D. and Langmuir C. H. (1996) The boron systematics of intraplate lavas: Implications for crust and mantle evolution. *Geochim. Cosmochim. Acta* **60**, 415–422.

Saal A. E., Hauri E. H., Langmuir C. H. and Perfit M. R. (2002) Vapour undersaturation in primitive mid-ocean-ridge basalt and the volatile content of Earth's upper mantle. *Nature* **419**, 451–455.

Schilling J.-G. (1973) Iceland mantle plume: Geochemical study of Reykjanes Ridge. *Nature* **242**, 565–571.

Schilling J.-G., Bergeron M. B., Evans R. and Smith J. V. (1980) Halogens in the Mantle Beneath the North Atlantic. *Philos. Trans. R. Soc. Lond. Ser. A* **297**, 147–178.

Schilling J.-G., Zajac M., Evans R., Johnston T., White W., Devine J. D. and Kingsley R. (1983) Petrologic and geochemical variations along the Mid-Atlantic Ridge from 29 degrees N to 73 degrees N. *Am. J. Sci.* **283**, 510–586.

Shishkina T. A., Botcharnikov R. E., Holtz F., Almeev R. R., Jazwa A. M. and Jakubiak A. A. (2014) Compositional and pressure effects on the solubility of H_2O and CO_2 in mafic melts. *Chem. Geol.* **388**, 112–129.

Shishkina T. A., Botcharnikov R. E., Holtz F., Almeev R. R. and Portnyagin M. V. (2010) Solubility of H_2O- and CO_2-bearing fluids in tholeiitic basalts at pressures up to 500 MPa. *Chem. Geol.* **277**, 115–125.

Shorttle O. and Maclennan J. (2011) Compositional trends of Icelandic basalts: Implications for short-length scale lithological heterogeneity in mantle plumes. *Geochem. Geophys. Geosyst.* **12**, Q11008. https://doi.org/10.1029/2011GC003748.

Shorttle O., Maclennan J. and Lambart S. (2014) Quantifying lithological variability in the mantle. *Earth Planet. Sci. Lett.* **395**, 24–40.

Shorttle O., Maclennan J. and Piotrowski A. M. (2013) Geochemical provincialism in the Iceland plume. *Geochim. Cosmochim. Acta* **122**, 363–397.

Shorttle O., Moussallam Y., Hartley M. E., Maclennan J., Edmonds M. and Murton B. J. (2015) Fe-XANES analyses of Reykjanes Ridge basalts: Implications for oceanic crust's role in the solid Earth oxygen cycle. *Earth Planet. Sci. Lett.* **427**, 272–285.

Skovgaard A. C., Storey M., Baker J., Blusztajn J. and Hart S. R. (2001) Osmium-oxygen isotopic evidence for a recycled and strongly depleted component in the Iceland mantle plume. *Earth Planet. Sci. Lett.* **194**, 259–275.

Smith H. J., Spivack A. J., Staudigel H. and Hart S. R. (1995) The boron isotopic composition of altered oceanic crust. *Chem. Geol.* **126**, 119–135.

Sobolev A. V., Hofmann A. W., Kuzmin D. V., Yaxley G. M., Arndt N. T., Chung S.-L., Danyushevsky L. V., Elliott T., Frey F. A., Garcia M. O., Gurenko A. A., Kamenetsky V. S., Kerr A. C., Krivolutskaya N. A., Matvienkov V. V., Nikogosian I.

K., Rocholl A., Sigurdsson I. A., Sushchevskaya N. M. and Teklay M. () The amount of recycled crust in sources of mantle-derived melts. *Science* **316**, 412–417.

Spivack A. J. and Edmond J. M. (1987) Boron isotope exchange between seawater and the oceanic crust. *Geochim. Cosmochim. Acta* **51**, 1033–1043.

Steele-MacInnis M., Esposito R. and Bodnar R. J. (2011) Thermodynamic model for the effect of post-entrapment crystallization on the H_2O-CO_2 systematics of vapor-saturated, silicate melt inclusions. *J. Petrol.* **52**, 2461–2482.

Stracke A. (2012) Earth's heterogeneous mantle: A product of convection-driven interaction between crust and mantle. *Chem. Geol.* **330**, 274–299.

Stracke A., Zindler A., Salters V. J. M., McKenzie D., Blichert-Toft J., Albaréde F. and Grönvold K. (2003) Theistareykir revisited. *Geochem. Geophys. Geosyst.* **4**, 8507. https://doi.org/10.1029/2001GC000201.

Tanaka R. and Nakamura E. (2005) Boron isotopic constraints on the source of Hawaiian shield lavas. *Geochim. Cosmochim. Acta* **69**, 3385–3399.

Thirlwall M. F., Gee M. A. M., Taylor R. N. and Murton B. J. (2004) Mantle components in Iceland and adjacent ridges investigated using double-spike Pb isotope ratios. *Geochim. Cosmochim. Acta* **68**, 361–386.

Vils F., Tonarini S., Kalt A. and Seitz H.-M. (2009) Boron, lithium and strontium isotopes as tracers of seawater–serpentinite interaction at Mid-Atlantic ridge, ODP Leg 209. *Earth Planet. Sci. Lett.* **286**, 414–425.

Walowski K. J., Kirstein L. A., De Hoog J. C. M., Elliott T. R., Savov I. P., Jones R. E. and EIMF (2019) Investigating ocean island mantle source heterogeneity with boron isotopes in melt inclusions. *Earth Planet. Sci. Lett.* **508**, 97–108.

Weaver B. L. (1991) Trace element evidence for the origin of ocean-island basalts. *Geology* **19**, 123–126.

White W. M. (1985) Sources of oceanic basalts: Radiogenic isotopic evidence. *Geology* **13**, 115–118.

White W. M. (2010) Oceanic island basalts and mantle plumes: the geochemical perspective. *Annu. Rev. Earth Planet. Sci.* **38**, 133–160.

White W. M. (2015) Probing the Earth's deep interior through geochemistry. *Geochem. Perspect.* **4**.

White W. M. and Hofmann A. W. (1982) Sr and Nd isotope geochemistry of oceanic basalts and mantle evolution. *Nature* **296**, 821.

Winpenny B. and Maclennan J. (2011) A partial record of mixing of mantle melts preserved in icelandic phenocrysts. *J. Petrol.* **52**, 1791–1812.

Wood D. A., Joron J. L., Treuil M., Norry M. and Tarney J. (1979) Elemental and Sr isotope variations in basic lavas from Iceland and the surrounding ocean floor: Nature of mantle source inhomogeneities. *Contrib. Miner. Petrol.* **70**, 319–339.

Workman R. K. and Hart S. R. (2005) Major and trace element composition of the depleted MORB mantle (DMM). *Earth Planet. Sci. Lett.* **231**, 53–72.

Workman R. K., Hauri E., Hart S. R., Wang J. and Blusztajn J. (2006) Volatile and trace elements in basaltic glasses from Samoa: Implications for water distribution in the mantle. *Earth Planet. Sci. Lett.* **241**, 932–951.

Yang H.-J., Kinzler R. J. and Grove T. L. (1996) Experiments and models of anhydrous, basaltic olivine-plagioclase-augite saturated melts from 0.001 to 10 kbar. *Contrib. Miner. Petrol.* **124**, 1–18.

Zindler A. and Hart S. (1986) Chemical geodynamics. *Annu. Rev. Earth Planet. Sci.* **14**, 493–571.

Zindler A., Hart S. R., Frey F. A. and Jakobsson S. P. (1979) Nd and Sr isotope ratios and rare earth element abundances in Reykjanes Peninsula basalts evidence for mantle heterogeneity beneath Iceland. *Earth Planet. Sci. Lett.* **45**, 249–262.

Associate editor: Andreas Stracke